MASTER IN BIOMEDECINE

Investigation of ABCB9 and ABCB6 localization and mierization in different cell lines

Bailly, Julie

Award date:
2021

Awarding institution:
University of Namur

Faculté de Médecine

INVESTIGATION OF ABCB9 AND ABCB6 LOCALIZATION AND DIMERIZATION IN DIFFERENT CELL LINES

Mémoire présenté pour l'obtention

du grade académique de master en sciences biomédicales

Julie BAILLY

Janvier 2021

Université de Namur
FACULTE DE MEDECINE
Secrétariat des départements
Rue de Bruxelles 61 – 5000 NAMUR
Téléphone : +32(0)81.72.43.22
Email : – manon.chatillon@unamur.be – http://www.unamur.be/

Investigation of ABCB9 and ABCB6 localization and dimerization in different cell lines

BAILLY Julie

Abstract:

BACKGROUND – ATP-binding cassette (ABC) transporters represent the largest superfamily of transmembrane proteins composed of 48 transporters divided into seven families, named from A to G. ABC transporters have been extensively studied for their implication in chemoresistance. In the past decade, they received more attention for their potential role in tumor biology, which led to unravel their role in tumor development and progression. The ABCB family is composed of four full-transporters and eight half-transporters, which must either homo- or heterodimerize to become functional. This research project focuses on ABCB6 and ABCB9, two half ABCB transporters, which were previously shown to heterodimerize in engineered HEK293T cells using co-immunoprecipitation and NanoBRET.

AIMS – This study aims to further investigate the heterodimerization of ABCB6 and ABCB9 in three different cell lines, which we hypothesize they constitutively express them.

METHODS –RT-qPCR and western blot were used to study the mRNA and protein expression of ABCB6 and ABCB9 in the 3 chosen cell lines, which are the MDA-MB-231 breast cancer cell line, the MDA-MB-435 melanoma cell line, and the immortalized Sertoli cells. Then, subcellular fractionation was used to investigate the localization of both transporters in MDA-MB-231 and MDA-MB-435 cell lines. Lastly, co-immunoprecipitation was performed to study their potential heterodimerization.

RESULTS – mRNA and protein expression of ABCB6 and ABCB9 have been detected in each cell lines except protein expression of ABCB6, which was not detected in the Sertoli cells. Regarding the localization, both transporters have been localized in the soluble cytosolic fraction, which gave rise to many questions as they are both transmembrane proteins. We were not able to show the heterodimerization of ABCB6 and ABCB9 using co-immunoprecipitation.

CONCLUSION – ABCB6 and ABCB9 are both expressed at the mRNA and protein levels in MDA-MB-231 and MDA-MB-435 cell lines. In Sertoli cells, ABCB6 was not expressed at the protein level, whereas ABCB9 mRNA and protein were detected. The localization of both transporters remains to be investigated, as they were recovered mainly in the cytosolic fraction. Lastly, the heterodimerization of ABCB6 with ABCB9 could not be validated.

Keywords: ABC transporters, ABCB6, ABCB9, Multidrug resistance, localization, dimerization

Mémoire de master en sciences biomédicales
Janvier 2021
Thesis supervisor : Jean-Pierre Gillet

Acknowledgments

First, I would like to thank Professor Gillet and Louise Gerard, for all their corrections, the time they gave me and everything they taught me. As well as all the members of the LBMC laboratory for welcoming me in it.

I thank, Professor Boonen, Florentine Gilis, Virginie Tevel, for all their advises and help with the fractionation. As well as Martine Albert for her kindness and help when I was overwhelmed.

I also thank my open space buddies, Laurent Duvivier, Maxence Toussaint, Céline Bidron, Adriana Maria Diaz Anaya, Degan and Thomas. I'm going to miss all the restaurants, take away, karaoke, aperitivos and chit chat. I'm so grateful for having you by my side during this thesis, you gave me unconditional moral support.

A big thank to my rugby club, Rugby Haute Meuse (RHM), more particularly, Martin, for taking such a good care of me. Lionel and Charlotte, for all the support and running. But also, to the best team, les Biches, with who we would have win the cup this year if it wasn't for the corona crisis.

Thank you, to Camille, Marion and Christel, my master buddies. I'm lucky to have you in my life, whether to laugh or cry. But also, to Antoine, my best friend, who have been here for me to support (almost) every of my decisions during the past 3 years.

Last but not least, I would like to thank my parent and family. It hasn't been easy every day to live so far away from you, but you have always supported me and helped me in the best way. I'm lucky to have such a wonderful loving family.

Table des matières

Abbreviations

ABC : ATP binding cassette

ABC-me : ABC-mitochondrial erythroid

ALK : Anaplastic lymphoma kinase

ATP : Adenosine Triphosphate

BSEP : bile salt export pump

Co-IP : Co-immunoprecipitation

DDR : DNA damage repair

EGFR : Epidermal growth factor receptor

EMT : epithelial mesenchymal transition

GSH : glutathione

HCC : Hepatocellular carcinoma

HoC : Hallmarks of cancer

IAP : Inhibitors of apoptosis

IF : inward-facing

LAMP : Lysosomal associated membrane protein

mBu : milli-bioluminescence

MDR : multidrug resistance

MHC : major histocompatibility complex

OF : outward facing

NanoBRET : Nano Bioluminescence Resonance Energy Transfer

NBD : Nucleotide Binding Domain

NSCLC : Non-small-cell lung cancer

PCD : programmed cell deaths

PRP : P-glycoprotein-related protein

RT-qPCR : Reverse transcriptase – quantitative Polymerase chain reaction

Sh-RNA : short hairpin RNA

TAP : Transporters associated with antigen processing

TAP-L : Transporter associated with antigen processing-like

TMD : Transmembrane Domain

UR : unlocked-return

WB : Western blot

1 Introduction

1.1 ABC transporters

1.1.1 Generalities

ATP-binding cassette (ABC) transporters represent the largest superfamily of transmembrane proteins composed of 48 transporters. They are divided into seven families, named from A to G, based on their structures and sequences [1, 2]. ABC transporters are primary active transporters, they use ATP hydrolysis to transport molecules against their chemical gradient across membranes [3]. In eukaryotes, ABC transporters are exporters, they transport molecules from the cytoplasm to the extracellular environment or into organelles (e.g. endoplasmic reticulum, lysosome, mitochondria) [2]. In prokaryotes, they function mostly as importers in order to transport molecules for which diffusion is not possible [2, 4]. In human, these transporters export numerous substrates, such as amino acids, ions, oligonucleotides, sugar, lipids, toxins, drugs… through lipid membranes [3, 4]. Among families, some recurrence of substrate can be found (**Table 1**).

ABC family	Substrates
ABCA	Lipids Xenobiotics (ABCA2-3-6)
ABCB	Xenobiotics (ABCB1-5-6) Peptide (ABCB2-3-8-10) Iron (ABCB6) Fe/S cluster (ABCB7) Lipids (ABCB4) Bile Salt (ABCB11)
ABCC	Xenobiotics (ABCC1-3-10-11-12) Organic anion (ABCC2) Nucleoside (ABCC4-5)
ABCD	Fatty acids
ABCG	Steroids (ABCG1-5-8) Xenobiotics (ABCG2)

Table 1 – Overview of substrate specificity in ABC transporter family, ABCE and F are not mentioned because they are more likely to play a role of regulators rather than a role of transporters [5-7].

The transport of those molecules ensures physiological functions including elimination of waste products, cellular lipid transport, cell signaling, uptake of nutrients and energy generation [8, 9]. It must be noted that not all ABC transporters act as a transporter moving substrates. For example, some ABC proteins, such as ABCC7, act as ion channels regulator [10]. Moreover, ABCE and ABCF are described as transcription factors or regulatory proteins because of their atypical conformation, as described in the following paragraph [11].

1.1.2 Structure

The typical conformation of an ABC transporter is two nucleotide binding domains (NBD) and two transmembrane domains (TMD) (**Figure 1A**) [1, 8]. In eukaryotes, those four domains are constituted by a single polypeptide. In bacteria, different combinations are possible : individual polypeptide, a combination of fused NBD and/or TMDs or pairwise identical subunits [3]. NBD is a key feature of an ABC transporter as it is composed of highly conserved domains throughout families [4, 8]. The NBD contains different motifs, Walker A (P-loop) and B, an α-helical domain with the ABC signature LSGGQ and some characteristic motifs including A-,Q-, and D-loops (**Figure 1B**) [3, 8, 12].The main role of NBD is ATP binding and hydrolysis, to do so the two cytosolic NBDs interact with each other forming a head-to-tail dimer [13, 14]. ATP molecules bind to the dimer interface, interacting with the Walker A motif of one NBD and the ABC signature LSGGQ of the other NBD [14]. On the opposite, TMDs have different characteristics depending on the transporter, but their core are most of the time composed of six α-helices [3, 12]. Those α-helices form the ligand binding site that recognizes and transports specific substrates, giving its specificity to the transporter [8].

Beside the typical full ABC transporter described above, which are composed of two TMD and two NBD encoded as a single polypeptide chain, half transporters also exist (**Figure 1A**). They are formed of one NBD and one TMD. To be functional, an half transporter needs to homo- or heterodimerize [12]. Three ABC families comprise half transporters: ABCB contains 8 half-transporters (ABCB 2-3, 5β, 6-10), ABCD has 4 (ABCD1-4) and ABCG counts 5 half transporters (ABCG1, 2, 4, 5, 8) with the particularity of having a reversed topology compared to the B and D families. Indeed, the NBD is located at the N-terminal side instead of the C-terminal one (**Figure 1A**) [2, 9, 15]. Other particularities exist, for instance, certain ABCC (ABCC1-3,6,8-10) and ABCB transporters (ABCB6, ABCB9) have a third TMD, called TMD0, either on their N-terminus or C-terminus side (**Figure 1A**) [15-17]. It must also be noted that transporters of the ABCE and F families are only composed of two NBD and lack the transmembrane domain, which implies that their function is different from a conventional transporter [11].

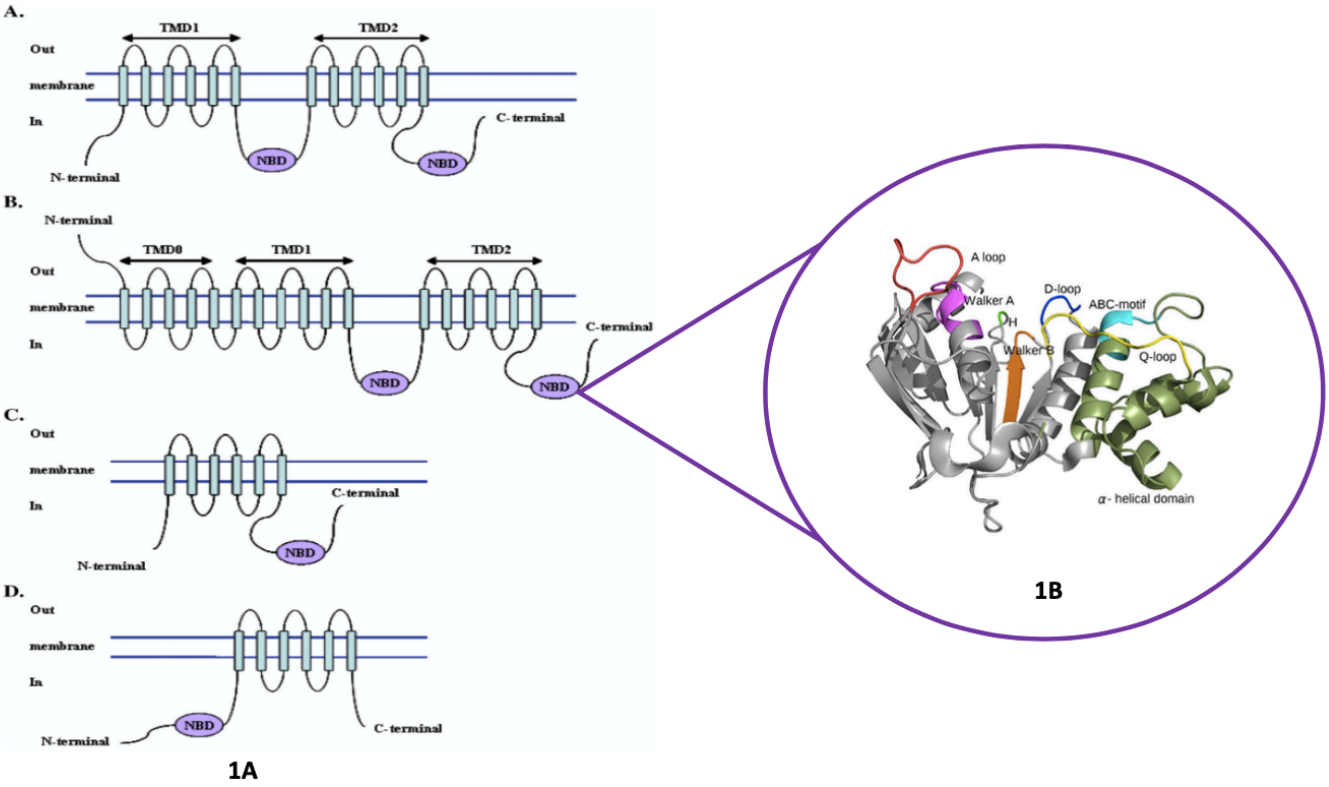

Figure 1 - Structure of ABC transporters. 1A. (A) Typical structure of ABC transporters, 2 transmembrane domains (TMD) and 2 nucleotide binding domains (NBD). (B) Some ABC transporters (i.e. ABCC1-3,6,8-10, ABCB6, ABCB9) contain an additional TMD, called TMD0 composed of 5 alpha helices. (C) A typical half transporter with TMD at the N-terminal and NBD at C-terminal. (D) ABCG subfamily known to be reversed half transporter with TMD at the C-terminal and NBD at the N-terminal. **1B**. Structure of the nucleotide binding domain, the NBD contains different conserved motifs, Walker A (P-loop) and B, an α-helical domain with the ABC signature LSGGQ and some characteristic motifs including Q-, A- and D-loops. Adapted from Gillet *et al* and Genovese *et al*. [9, 18].

1.1.3 Catalytic cycle

In order to export molecules against their chemical gradient, an active turnover condition happens using ATP hydrolysis [3, 13]. Different conformations can be observed, inward-facing (IF), unlocked-return (UR) and outward-facing (OF) [13]. IF shows two distinct conformations itself, IF^{wide} and IF^{narrow}. The first one, IF^{wide} allows the intracellular gate to be wider, hence enabling the movement of transmembrane helix six (TM6) [13]. TM6 acts as a gatekeeper for the substrate binding, preventing the binding of unsuitable molecules. As the concentration of substrate increases, the equilibrium of IF^{wide} : IF^{narrow} change from 1:1 to 4:1 allowing substrate to bind to TMD [13]. Independently of substrate binding and IF conformation, ATP is going to bind to NBD, inducing NBD dimerization, which will close the intracellular gate and open the extracellular one [13]. Hence, the substrate will be released into the extracellular side and the conformation can either be OF^{open} or $OF^{occluded}$. After hydrolysis of one ATP, P_i will be released and give the asymmetric UR conformation triggering partial opening of the intracellular gate and the NBDs causing the exporter to going back to its initial state, IF^{narrow} (**Figure 2**) [13].

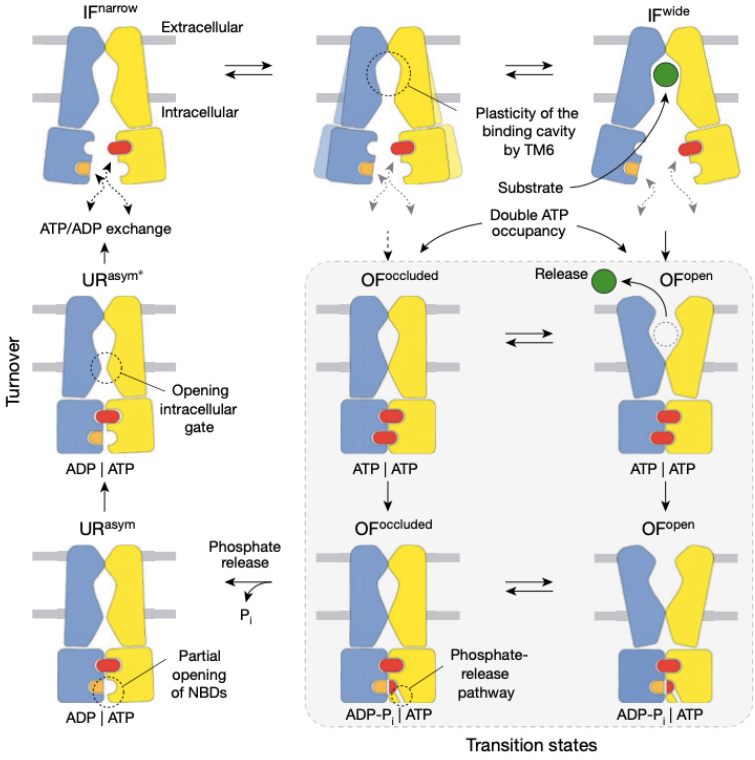

Figure 2 - ATP catalytic cycle of a full ABC transporter. Equilibrium between IF^{narrow} and IF^{wide} shifting to IF^{wide} due to the binding of the substrate. Different conformations possible: Inward-facing (IF), unlocked-return (UR) and outward-facing (OF). IF^{wide} allows the intracellular gate to be wider, allowing the movement of transmembrane helix six (TM6). TM6 acts as a gatekeeper for the substrate binding, preventing the binding of unsuitable molecules. As the concentration of substrate increases, the equilibrium of IF^{wide}: IF^{narrow} change allowing substrate to bind to TMD. Independently of substrate binding and IF conformation, ATP is going to bind to NBD, inducing NBD dimerization, which will close the intracellular gate and open the extracellular one. The substrate will be released into the extracellular side and the conformation can either be OF^{open} or $OF^{occluded}$. After hydrolysis of one ATP, P_i will be released and give the asymmetric UR conformation triggering partial opening of the intracellular gate and the NBDs causing the exporter to going back to its initial state, IF^{narrow}. Taken from Hofmann *et al* [13].

1.1.4 Disease implication

As mentioned, ABC transporters are involved in many different physiological processes by translocating many types of substrates. Therefore, their mutation can lead to a wide variety of human disorders (**Table 2**).

Disease	Transporter involved
Tangier disease	ABCA1
Various eye diseases	ABCA4
Bare lymphocyte syndrome	ABCB2/B3
Anemia and X-linked sideroblastomic anemia	ABCB7
Pseudoxanthoma elasticum	ABCC6
Adrenoleukodystrophy	ABCD1
Sitosterolemia	ABCG5/G8
Progressive familial intrahepatic cholestasis 3	ABCB4
Obstetric cholestasis	ABCB4
Progressive familial intrahepatic cholestasis 2	ABCB11
Porphyria	ABCB6
Dubin-Johnson syndrome	ABCC2
Cystic fibrosis	ABCC7
Persistent hyperinsulinemic hypoglycemia of infancy	ABCC8

Table 2 – Human diseases associated with ABC transporters [8]

For instance, porphyria is a disease caused, most of the time, by autosomal dominant mutations of genes coding for heme biosynthetic enzymes [19]. Those mutations lead to accumulation of cytotoxic metabolic porphyrin intermediates which damage the liver, skin, neural tissues and hematopoietic system. Most common symptoms are severe abdominal pain, nausea/vomiting, red or brown urine and constipation or diarrhea. ABCB6 has been identify as a genetic modifier of porphyria, meaning that its mutation has an impact on the severity of the disease. This can partially explain why this disorder displays a variable range of expressivity and penetrance in different patients [19]. Fukuda *et al.* showed, using deep sequencing, mouse model and biochemical analysis, that ABCB6 can ease porphyria severity by expelling porphyrins [19].

Nevertheless, ABC transporters can directly cause the disease as it is the case for sitosterolemia. It is an autosomal recessive disorder caused by a biallelic mutation in either *ABCG5* (Sterolin-1) or *ABCG8* (Sterolin-2) [20]. ABCG5 and ABCG8 heterodimerization is mandatory for their expression in the apical membrane of the intestine, liver and gallbladder [21]. A mutation in either transporter, affecting their dimerization, retains both transporters in the endoplasmic reticulum, which leads to a decreased biliary excretion of sterol and an increased intestinal absorption of sterols [20]. The increased sterols plasma level leads to xanthomas, accelerated atherosclerosis and coronary artery disease [20].

1.2 ABCB family

The ABCB family is the only family containing both full and half transporters. Indeed, it is composed of four full-transporters (i.e. ABCB1, ABCB4, ABCB5FL, ABCB11) and eight half-transporters (i.e. ABCB2-3, ABCB5β, ABCB6-10) with different physiological roles and features [11]. This family is mainly known for its implication in multidrug resistance (MDR).

ABCB1 is known as MDR1 or P-glycoprotein and is the first discovered ABC transporter [22]. Beside its role in MDR, ABCB1 is expressed in many tissues including the intestine, where it impacts the bioavailability of many drugs (e.g. digoxin and nelfinavir) but also in the blood-brain barrier where it has an important gatekeeper role [23].

ABCB2 and ABCB3, also known as TAP1 and TAP2, are endoplasmic reticulum membrane transporters that dimerize together and play a role in MHC I-dependent antigen presentation to cytotoxic T cells [11, 24].

ABCB4 is mainly localized in the liver, and is involved in biliary phospholipid secretion [11, 25]. It reduces the toxicity of bile salts by mediating the transport of phosphatidylcholine from the canalicular membrane of hepatocytes to the biliary pathway [11].

ABCB5 is expressed in many tissues such as testis, mammary tissue, melanocytes and retinal pigmented epithelium, but also in many cancers such as colorectal cancer, melanoma and breast cancer where it mediates multidrug resistance [26-30]. It is also a metastatic melanoma progression marker [31]. Based on AceView program, 11 different mRNAs have been identified [32]. Among those transcript variants, the longest three have been studied, ABCB5 Full length (FL), ABCB5β, and ABCB5α, [32]. ABCB5α encodes for a peptide of 15 kDa, which only contains an ABC signature and a walker B sequence, but no Walker A [29]. Because of its topology, ABCB5α is suspected to have a regulatory role instead of acting as a transporter [31].

ABCB5 transporter has evolved into a full transporter called ABCB5 Full length (FL) (1257 aa) [31]. It is mainly expressed in testis and prostate as well as in pigmented cells such as melanocytes [33, 34]. Its topological structure corresponds to the typical full ABC transporters structure described above. It shows a strong homology with ABCB1 [31, 33]. Keniya et al. have shown that ABCB5 FL mediates the resistance to several drugs such as rhodamine 123, daunorubicin and tetramethylrhodamine [35]. Another study conducted by Kawanobe and colleagues has shown that ABCB5FL confers resistance to docetaxel and paclitaxel as well as doxorubicin and other drugs [34].

ABCB5β (812 aa) differs from the other ABCB half transporters [36]. Indeed, it contains 6 transmembrane α-helices forming the TMD, but it has two NBD instead of one [31]. However, the NBD on the N-terminal is lacking a walker A sequence giving a unique feature to ABCB5β [31]. Beside this particularity, potential dimerization sites in the N-terminal region in TMD have been identified, which are expected to allow ABCB5β to dimerize and to form a functional transporter [31]. Keniya and colleagues, showed that compared to ABCB5FL, ABCB5β homodimer does not confer drug resistance to several compounds [35]. Therefore, we hypothesized that ABCB5β works as a heterodimer to fulfill its transporter function.

ABCB7, ABCB8 and ABCB10 are mitochondrial transporters. ABCB7 is localized in the inner membrane of mitochondria and is involved in the transport of iron and sulfur [36]. This transporter is known mostly for its implication in X-linked sideroblastic anemia where an accumulation of iron is observed [37]. ABCB8 is a mitochondrial K_{ATP} channel involved in MDR as it exports doxorubicin. It regulates the transport of potassium (K^+), iron and glutathione (GSH) and has a cardioprotective role against oxidative stress [36]. ABCB10 also known as ABC-me (ABC-mitochondrial erythroid) protects the cell from increased oxidative stress associated with heme metabolism [36].

ABCB11 known as bile salt export pump (BSEP) is also involved in the excretion of bile salt into the bile like ABCB4 [38].

This research project will focus on ABCB6 and ABCB9, described below.

1.3 ABCB9

ABCB9, named as the transporter associated with antigen processing-like (TAPL), is a half transporter that has to dimerize to translocate peptides from the cytosol into the lumen of lysosomes [39]. Its structure is different from a typical half transporter as it contains an extra N-terminal transmembrane domain called TMD0 (**Figure 3**) [39]. This accessory TMD0 is needed for lysosomal targeting and for interaction with membrane proteins associated with lysosome, such as LAMP-1/2 [39].

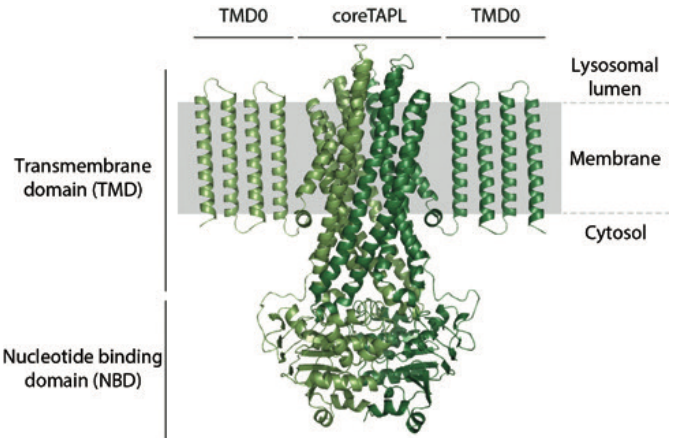

Figure 3 – Structure of TAPL homodimer. Core TAPL is composed of 2 TMD and 2 NBD as described in section 1.1.2. This half transporter contains an additional N-terminal transmembrane domain (TMD0). TMD0 is composed of four transmembrane helices. Image taken from Zollman *et al.* [40].

Its name comes from its sequence homology with TAP1 and TAP2, indeed they share 38% and 40% amino acid sequence identity [39]. Phylogenic analyses have suggested that TAPL is the common ancestor of the TAP family as its evolving rate is slower than the one of TAP1 and TAP2 [41]. This can explain the homology between ABCB9 of mouse and rat (99%) and also between rodents and human (95%) [41].

TAPL gene consists of 12 exons on human chromosome 12q23.34, encoding the longest isoform defined as 12A [42]. Kobayashi *et al.* have identified two additional TAPL isoforms termed 12B and 12C [42]. After a southern blot analysis, the assumption was made that the

transcripts are produced by alternative splicing of the 12th exon of TAPL gene [42, 43]. They are all transcribed, even though transcript 12A seems to be the one that is transcribed the most [42]. Using 3'RACE, they noticed that 12B and 12C have shorter carboxyl terminal sequences compared to 12A [42]. This difference in length could affect the specificity and efficiency of TAPL as a transporter [42].

Even though the physiological role of TAPL is still elusive, in 2005, Wolters *et al.* have found the first evidence that homodimer of TAPL transports peptides [44]. They used crude membranes from sf9 insect cells expressing TAPL and radiolabeled peptides library to screen peptide specificity [44]. Unlike TAP, TAPL translocates a broader length specificity peptides, ranging from 6-mer to 59 residues [39]. Usually, ABC transporters export hydrophobic peptides (drugs, cholesterol, …), but ABCB9 was shown to transport hydrophilic peptides [39, 40]. Studies have been performed to assess whether TAPL has similar function regarding MHC-I dependent antigen presentation like TAP1 and TAP2 [41]. Kobayashi *et al.,* using semi-quantitative PCR, highlighted that unlike TAP1 and TAP2, TAPL mRNA level did not change after the addition of interferon ɣ in the cell culture [41]. This observation showed that TAPL gene is not regulated by interferon ɣ like TAP1 and TAP2 [41].

Different studies have localized ABCB9 in the lysosome, but it remains controverted in the literature and its possible localization in the endoplasmic reticulum has also been highlighted [41, 45]. Orthologues of ABCB9 can be found in vacuoles and lysosome like compartments in plants and invertebrates, supporting the hypothesis of localization in the lysosome [46]. Demirel *et al.* have studied the importance of TMD0 and core TAPL and their subcellular localization using immunofluorescence. They used transiently transfected HeLa cells and showed that wild type ABCB9 has a strong colocalization with LAMP2. However core-TAPL did not show the same results since it was mostly found at the plasma membrane [47]. Surprisingly, TMD0 expressed alone is localized in the lysosome, which lead to the hypothesis that TMD0 escorts core-TAPL to the lysosome [47]. The same study showed that core TAPL is sufficient and essential for peptide transport, and does not need the presence of TMD0.

ABCB9 was found to be highly expressed in testis, more particularly in Sertoli cells as well as in dendritic cells and macrophages [39]. Studies showed that it was upregulated during the maturation of monocytes [39]. It has been shown that ABCB9 is upregulated in paclitaxel-resistant breast cancer cells and seems to be involved in the regulation of oxaliplatin-based chemosensitivity in hepatocellular carcinoma [48, 49]. On the contrary, ABCB9 is downregulated in colorectal cancer [50]. Beside those observations, ABCB9 is a transporter that needs to be further characterize.

1.4 ABCB6

ABCB6 is a half transporter that contains an additional transmembrane domain, TMD0, like ABCB9, which is essential for its stability and function [16]. ABCB6 is also called, P-glycoprotein-related protein (PRP) because it has been discovered in 1997, while Furuya *et al.* were screening for novel ABC transporter genes associated with drug resistance in liver [16, 51]. They showed that its sequence was highly conserved and shared similarity to the yeast heavy metal transporter (hmt1) [51]. Since then, ABCB6 was further characterized and shown to be involved in resistance to toxic metals, in promoting tumor growth, in acquired drug resistance, and in protection against oxidative and phenyl hydrazine stress [16].This transporter is also known to transport porphyrins which is involved in heme biosynthesis. A study conducted by Fukuda *et al.*, showed that defective ABCB6 alleles are strongly associated with disease intensification of porphyria. Porphyria results in a build-up of cytotoxic porphyrin intermediates which lead to damages in the liver, haematopoietic system, skin and neural tissues [19].

ABCB6 localization in the literature is also controverted. It has been first localized in the mitochondrial membrane using subcellular localization and confocal microscopy [52]. Then, Paterson *et al.* further characterized ABCB6 by observing that depending on the cellular type this transporter could be either in the mitochondria or in the plasma membrane [53]. They also showed, using digitonin solubilization, that ABCB6 resided more precisely in the outer membrane [53]. The fact that mature red blood cells are lacking mitochondria led to the observation of ABCB6 in their membrane. This finding by Helias *et al.* gave the opportunity to understand the rare recessively inherited Lan blood group [16]. Afterwards in 2012, Kiss *et al.* also studied ABCB6 localization and they showed, using confocal microscopy and subcellular fractionation, that ABCB6 was localized in the endolysosomal compartment [54].

A study showed that the overexpression of ABCB6 was linked to the incomplete response to treatment in breast cancer [55]. They analyzed the expression profile of several ABC transporters in breast cancer patients treated with sequential weekly paclitaxel/FEC (5-Fluorouracil, epirubicin, and cyclophosphamide) neoadjuvant chemotherapy. They concluded that the ABC transporter gene expression profiling could be useful to predict response to specific treatments in breast cancer patients [55].

1.5 Chemoresistance

1.5.1 Generalities

Resistance remains the main obstacle to cancer treatment [56]. Resistance is mediated by several overlapping mechanisms either intrinsically present or acquired by cancer cells following treatment [57, 58]. Those mechanisms can be classified into different categories described below such as epigenetics, drug target alteration, drug inactivation, drug efflux (altered cellular pharmacology), DNA damage repair, cell death inhibition and epithelial mesenchymal transition (**Figure 4**) [59]. They can act independently or in combination, and are facilitated by other processes such as cancer cell heterogeneity, increased rate of genetic or epigenetic alteration, robust and redundant cell survival pathways and dynamic changes in time and space [58].

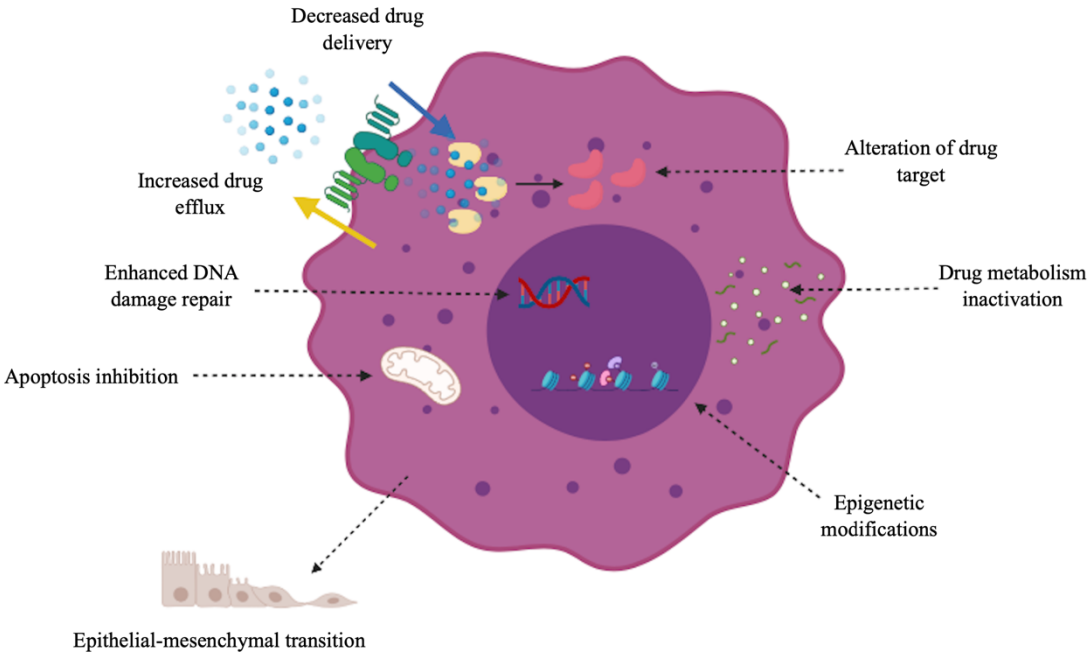

Figure 4 – Overview of the mechanisms involved in chemoresistance in a cancerous cell. This includes increased drug efflux, alteration of drug target, drug metabolism inactivation, epigenetic modifications, epithelial-mesenchymal transition (EMT) and enhanced DNA damage repair. Figure created with BioRender.com.

Two main types of **epigenetic modifications** can influence carcinogenesis, DNA methylation and histone modification via methylation or acetylation. These mechanisms can regulate the expression of different genes. For example, hypomethylation leads to overexpression of oncogenes promoting cancer cells survival and progression [59].

The **alteration of the drug target** is another mechanism promoting drug resistance as the efficacy of a drug is influenced by its target. This is well exemplified by the mutation of EGFR in lung cancer [60]. Indeed, anaplastic lymphoma kinase (ALK)-rearranged non-small-cell lung cancer (NSCLC) is known to be highly sensitive to crizotinib treatment but some cells become resistant through different mechanisms including mutation or amplification of EGFR, which is crizotinib's target [60].

Drug metabolism inactivation – Drug activation through metabolism is required for many anticancer agents in order to have a clinical efficacy [59]. Cytochromes P450 (CYPs) are key enzymes in activation and inactivation of anticancer drugs. Nevertheless, cancer cells may develop resistance to treatment by decreasing drug activation. For instance, in patients with advanced ovarian cancer, where they undergo treatment with platinum and taxane-based chemotherapy post-operatively, resistance to platinum occurs via drug inactivation by metallothioneins and thiol gluthatione, which activate the detoxification system [59].

DNA damage repair (DDR) plays an important role in anticancer drug resistance. Chemotherapeutics' aim is to cause direct or indirect damages to DNA, where DDR mechanisms can reverse those damages, which nullify the drug action [59].

Apoptosis and autophagy inhibition are two mechanisms used by cancer cells to avoid cell death. Inhibitors of apoptosis (IAPs) are proteins playing a significant role in the control of programmed cell deaths (PCD). PCD is essential to maintain healthy cell turnover in tissues and to fight infection or disease. It has been observed that cancer cells have increased expression of IPAs, which improves cell survival, enhances tumor growth and increases metastasis. Targeting IAPs has become interesting to re-sensitize cancer cells to chemotherapy and antibody-based therapy [61]. Regarding autophagy, its reduction contributes to tumor initiation, and its increase allows cancer cells to survive under hypoxia and metabolic stress conditions [62]. Its role in cancer is a bit contradictory as it can act either as a tumor suppressor pathway inhibiting tumor initiation, or as a drug resistance mechanism by facilitating cancer cell survival when anticancer drugs causes metabolic stresses [63].

Epithelial-mesenchymal transition (EMT) happens when epithelial cells lose their polarized organization and cell-to-cell junctions, as they develop a fibroblast-like morphology which increases their motility and invasive capacity [63]. This transition is driven by many different transcription factors regulating the expression of proteins involved in cell-to-cell contact, cell polarity, extracellular matrix (ECM) degradation and cytoskeletal structure [63]. Yao *et al.* has shown that cells undergoing EMT were resistant to EGFR inhibitors [64].

Drug efflux is one of the most studied mechanisms of cancer drug resistance. It is based on the reduction of drug accumulation in the cell by enhancing efflux of it. This mechanism will be described below as it implies the ABC transporters [59].

1.5.2 ABC transporter-mediated multidrug resistance

ABC drug efflux transporters have been largely described for their implication in multidrug resistance (MDR) [9]. MDR happens when cancer cells develop resistance against different anticancer drugs even though they are structurally and functionally unrelated [1, 65]. MDR is responsible for many deaths in cancer patients treated with chemotherapeutics [66].

Because of their implication in MDR, several ABC transporters have been named according to this. For example, ABCB1 is called multidrug resistance protein 1 (MDR1) and is known to transport a wide variety of chemotherapeutic agents such as Doxorubicin, Vinblastine, Paclitaxel and others [67]. The expression of ABCB1 is increased in many different cancers, such as in colon, kidney and ovary tumors, because of repeated drug treatment [18]. For instance, it has been shown that the expression of ABCB1 can be increased up to 1000-fold in lung cancer after exposition to Paclitaxel [18]. ABCC1 (MRP1-Multidrug resistance-associated protein 1) is also overexpressed in many different cancers, such as acute lymphoblastic

leukemia (ALL), acute myeloid leukemia (AML), breast, brain, pancreatic, non-small cell lung carcinoma, small cell carcinoma and prostate cancer [68]. ABCG2 (BCRP-Breast cancer resistance protein) is another ABC transporter, which was discovered in 1998 in a breast cancer cell line resistant to a range of cytotoxic agents, including doxorubicin, daunorubicin, and mitoxantrone [69]. Although many cancers may co-express several ABC transporters, this breast cancer cell line does not express ABCB1 or ABCC1. Since then, overexpression of ABCG2 has been found in many drug resistant cancers, such as ovarian, colon, small cell lung, gastric carcinoma, etc. [69]

ABC transporters' inhibitors have reached clinical trials in the late nineties [18]. The first generation composed among others of verapamil, tamoxifen and cyclosporine A (CSA) have shown severe side effects at the concentration required for modulation of ABC transporters because of their low potency [9]. This is mainly due to their aspecificity [9, 70]. The second generation of compounds were analogs of the first one, containing valspodar (CSA analogue) and toremifene (tamoxifen analogue). Those were more specific and were used at lower concentrations which decreased the toxicity. Unfortunately, they inhibited the CYP450, which led to a decrease in metabolism of co-administrated drugs resulting in enhance cytotoxicity. Nowadays, the third generation of inhibitors (e.g. laniquidar and zosuquidar) are investigated. They do not affect cytochrome P450, but so far none of them have been approved to treat cancer [71, 72]. Until now, clinical trials using ABC inhibitors have not met the expectations, this can be explained by multiple reasons. First, in several assays, patients were not selected based on their expression of ABC transporters in tumor [73]. Then, ABC transporters are involved in numerous physiological functions, e.g. central nervous system protection, which render the development of an ABC transporters modulator challenging. Different groups have sought new techniques to get around ABC transporter inhibition. For example, using CRISPR-Cas9 technology to inhibit the DNA expression of ABCB1 in osteosarcoma. Knockout of ABCB1 could restore the sensitivity of osteosarcoma drug resistant cells to doxorubicin [74].

1.6 ABC transporters beyond their role in cancer drug resistance

Beside their role in chemoresistance, ABC transporters have been shown to play an important role in tumor development and progression [71]. Previously, studies related to cancer were focused on the characterization of the role of ABC transporters as drug-efflux transporters. In 2000, Hanahan and Weinberg highlighted six acquired capacities of cancer cells; insensitivity to anti-growth signals, apoptosis escape, self-sufficiency in growth signals, angiogenesis, metastasis and tissue invasion (**Figure 5**). Two other capacities were discovered later, evasion of immune surveillance and metabolic reprogramming [71, 75]. More recently, studies have been directed toward the implication of ABC transporters in the tumor biology, including cancer cell differentiation, proliferation, migration, and invasion [5]. It has become clear that ABC transporters are linked to a number of these hallmarks of cancer (HoC) and are correlated with a more aggressive phenotype and malignant progression [71].

One of the first study to demonstrate the link between tumorigenesis and ABC transporters was by Mochida and colleagues in 2003 [76]. They showed that the loss of ABCB1 hinders tumor progression and suppresses intestinal polyp formation in mice [76]. Tumor formation was four times lower in mice with P-gp knockout (KO) than in wild type mice, suggesting that P-gp has a role in tumor formation [76].

Another study showed that ABCC1 expression was correlated with differentiation grade, degree of microvascular invasion and tumor size in primary untreated hepatocellular carcinoma (HCC) [77]. They studied the transcriptional profile of ABCB1, ABCC1, ABCC3 and ABCG2 genes of 139 HCC patients, which showed that ABCC1 was the only transporter with an increased expression [77].

Metastasis and invasion – Gonzales and colleagues have shown that ABCB1 promoted metastasis. Indeed, they showed, using co-immunoprecipitation and confocal localization, that ABCB1 and CD44, which is a hyaluronan receptor involved in cell migration, are coregulated in cancer [78]. Another example is the downregulation of ABCG2 in the U251 glioblastoma cell line, which resulted in the inhibition of invasion and migration capacities of the cancer cells [79].

Anti-apoptosis – this hallmark is inevitably associated to MDR as cells that evade apoptosis render the drug ineffective. A good example is the presence of P-gp in the mitochondrial membrane of gastric cancer cells whereas in healthy adult gastric tissue, ABCB1 is silenced [80]. Healthy cells silence the expression of ABCB1 which lead to a greater level of cell death, highlighting the role of ABCB1 in blocking apoptosis in gastric cancer cells [80].

Sustained proliferation - In 2019, our laboratory revealed the role of ABCB5 as a tumor suppressor in melanoma [81]. Sana and colleagues showed that either mutation in ABCB5 or the loss of ABCB5 function lead to increased proliferative capacities and accelerates the development of melanoma [81]. Another study carried out by Chunyan *et al*. identified ABCG1 as a potential oncogene in lung cancer. ABCG1 is involved in the regulation of cholesterol homeostasis, which is essential for the function and survival of the cells [82]. They showed that ABCG1 was over-expressed in lung cancer and that it was involved in the regulation of cell proliferation and in apoptosis [82].

Inflammation - Some cancer types develop an inflammatory microenvironment to promote their proliferation and survival which support the angiogenesis and metastasis [71]. Important inflammation mediators, like prostaglandins, prostacyclin (PGI) and leucotriene C4 (LTC4) are transported by ABC transporters [71, 75].

Cancer stem cells – a subpopulation of cancer cells with the ability of self-renewal and differentiation properties results in tumour heterogeneity, which is a real challenge in cancer therapy [75]. ABCB1, ABCB5 and ABCG2 are highly expressed in cancer stem cells (CSC) [65]. Wilson *et al.* have shown that ABCB5 maintains malignant melanoma-initiating cells (MMIC) by controlling IL1β secretion [83]. When they inhibited ABCB5 in MMIC, they started to differentiate and reversed resistance occurred [83].

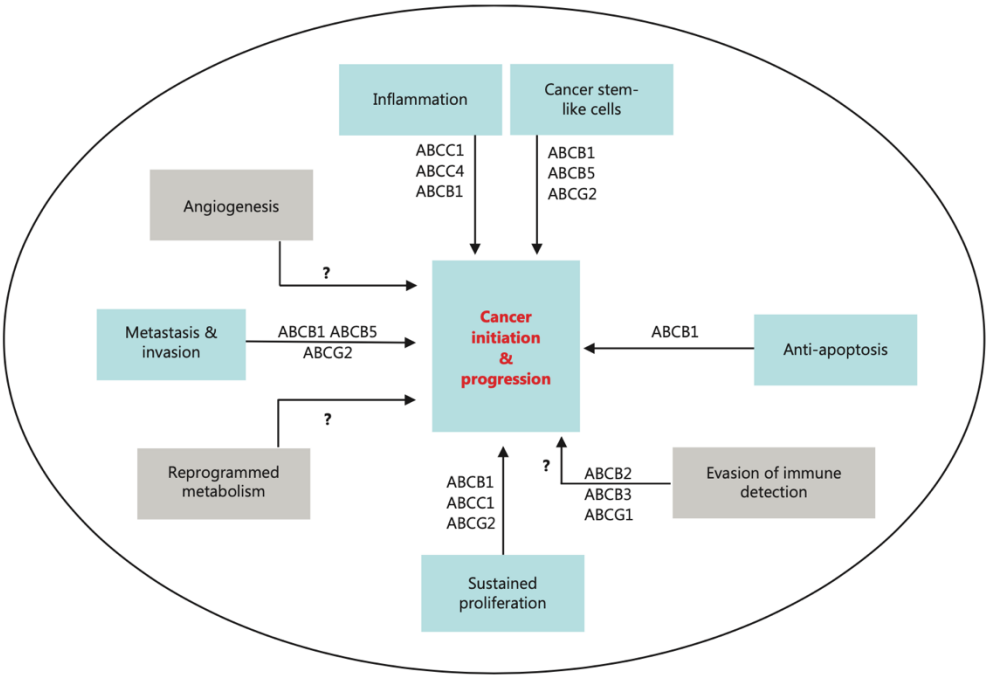

Figure 5 - ABC transporters involved in the different hallmarks of cancer. Some HoC, like angiogenesis and reprogrammed metabolism still need to be further investigated to be associated with dysregulation of ABC transporters [75]. Figure taken from Muriithi *et al.* [75].

2 Objectives

At first, this project focused on the investigation of the localization and heterodimerization of ABCB9 with ABCB5β in three different cell lines (i.e. MDA-MB-231 breast cancer cells, MDA-MB-435 melanoma cells, and immortalized Sertoli cells). The aim of our laboratory is to characterize ABCB5 to better understand its role in the biology of the cell and also in cancer. As we mentioned earlier, several transcript variants have been identified including ABCB5 FL and ABCB5 β, which encode a typical full transporter and a half transporter, respectively. ABCB5β and ABCB9 pair was selected based on preliminary data in HEK293T cell line showing their heterodimerization. This data had been generated by Simon Lefèvre using co-immunoprecipitation (**Figure 6**) and Louise Gerard using NanoBRET assay (**Figure 9**) [84, 85]. The co-immunoprecipitation was performed on HEK293T cells transfected with ABCB5β tagged with mCherry. The protein lysate was precipitated with either an anti-ABCB9 or anti-ABCB6 and the western blot was revealed with an anti-ABCB5 or an anti-mCherry (**Figure 6**).

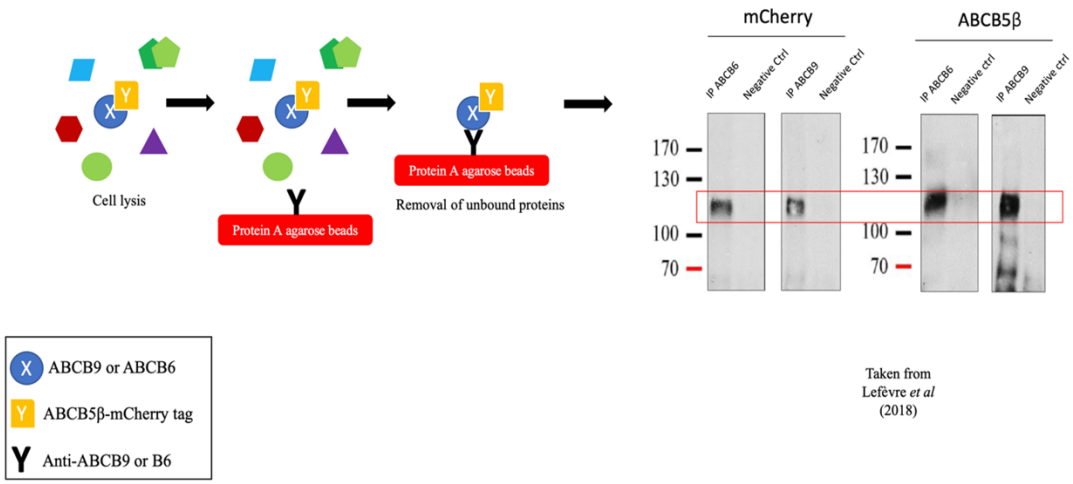

Figure 6 - Co-immunoprecipitation performed by precipitation of ABCB6 or ABCB9 followed by the revelation of ABCB5β mcherry fusion protein using an anti-mCherry antibody, or an anti-ABCB5 antibody. The band at 120 kDa, the expected size of the mcherry tagged-ABCB5β, highlight the heterodimerization of both transporters. This band is not present in the IgG controls (**negative ctrl**) [84]. Left panel inspired from mybiosource.com. Right panel taken from Simon Lefèvre *et al.* [84].

The Nano Bioluminescence Resonance Energy Transfer (NanoBRET) assay consists of a transfer of energy from a donor enzyme, NanoLuc, to an acceptor molecule, HaloTag labeled with HaloTag 618 ligand. NanoLuc is a luciferase, whereas HaloTag is a haloalkane dehalogenase [85]. During the assay, both proteins of interest are tagged with either NanoLuc or HaloTag in N ou C terminus, resulting in 4 genetic constructs. All possible combinations were tested, which result in 8 conditions (**Table 3**).

Pair 1	ABCB5β NanoLuc N – ABCB9 HaloTag N
Pair 2	ABCB5β NanoLuc N – ABCB9 HaloTag C
Pair 3	ABCB5β NanoLuc C – ABCB9 HaloTag N
Pair 4	ABCB5β NanoLuc C – ABCB9 HaloTag C
Pair 5	ABCB9 NanoLuc N – ABCB5β Halotag N
Pair 6	ABCB9 NanoLuc N – ABCB5β Halotag C
Pair 7	ABCB9 NanoLuc C – ABCB5β Halotag N
Pair 8	ABCB9 NanoLuc C – ABCB5β Halotag C

Table 3 – All possible combinations of ABCB5β and ABCB9 tagged either with NanoLuc or HaloTag in C- or N- terminal.

After NanoLuc substrate addition, if the donor and acceptor end up in close vicinity (<10 nm) due to protein-protein interaction, the donor will be able to transfer energy to the acceptor, which will emit luminescence at 610 nm (**Figure 7**). On the other hand, lack of interaction between the two proteins of interest will not allow acceptor emission (**Figure 7**).

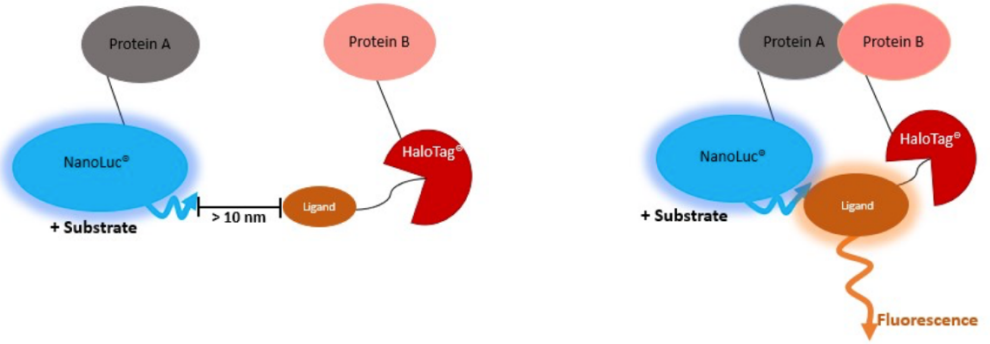

Figure 7 – Schematic representation of the NanoBRET. Energy transfer between the energy donor, NanoLuc protein fusion A and the energy acceptor, HaloTag protein of fusion B labeled with HaloTag 618 ligand. If NanoLuc and HaloTag are not closer than 10 nm the transfert of energy between the donor and acceptor will not occur. Figure taken from Louise Gerard *et al* [85].

To obtain a NanoBRET ratio in mBU (milli-bioluminescence units), the emission of the acceptor (at 610 nm) needs to be divided by the emission of the donor (at 447 nm) and multiplicate by 1000. The mean corrected mBU corresponds to the subtraction of the NanoBRET ratio of control sample without the 618 ligand and the sample with the ligand addition. Finally, the pair highlighting the biggest mean corrected mBU was selected for a donor saturation assay. The donor saturation assay allowed confirmation of the specificity of the interaction between both proteins. If a linear increase in signal is seen with growing amount of acceptor and constant amount of donor, it means that the signal is non-specific and comes from the overexpression of the construct in HEK293T cells. However, if a saturation is seen and the signal increases in a hyperbolic way, it means that all the donor are saturated with the acceptor due to a specific interaction (**Figure 8**).

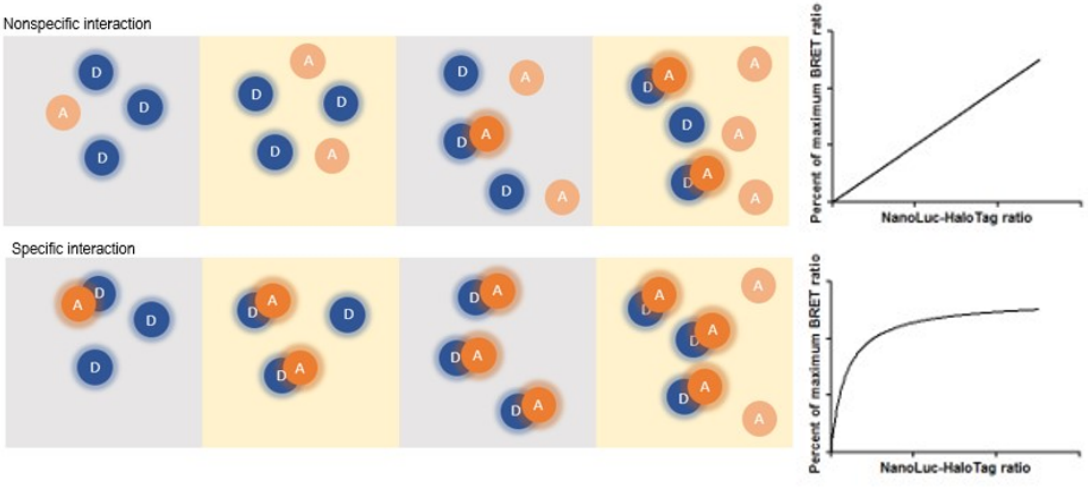

Figure 8 – Illustration of the Donor saturation assay. Determination of the specificity of interaction, increasing amount of acceptor is added (in orange) while the amount of donor is kept constant (in blue). Specific interaction will exhibit a saturation curve whereas nonspecific interaction will show a linear relationship. Figure taken from Louise Gerard et al [85].

ABCB5β and ABCB9 tagged with NanoLuc and HaloTag were tested using NanoBRET assay [85]. ABCB5β NanoLuc N with ABCB9 HaloTag N had the highest mean corrected mBU (**Figure 9**). As a result, this pair was chosen for the donor saturation assay, and a plateau was reached which confirmed that ABCB5β interaction with ABCB9 was specific, validating their heterodimerization (**Figure 9**).

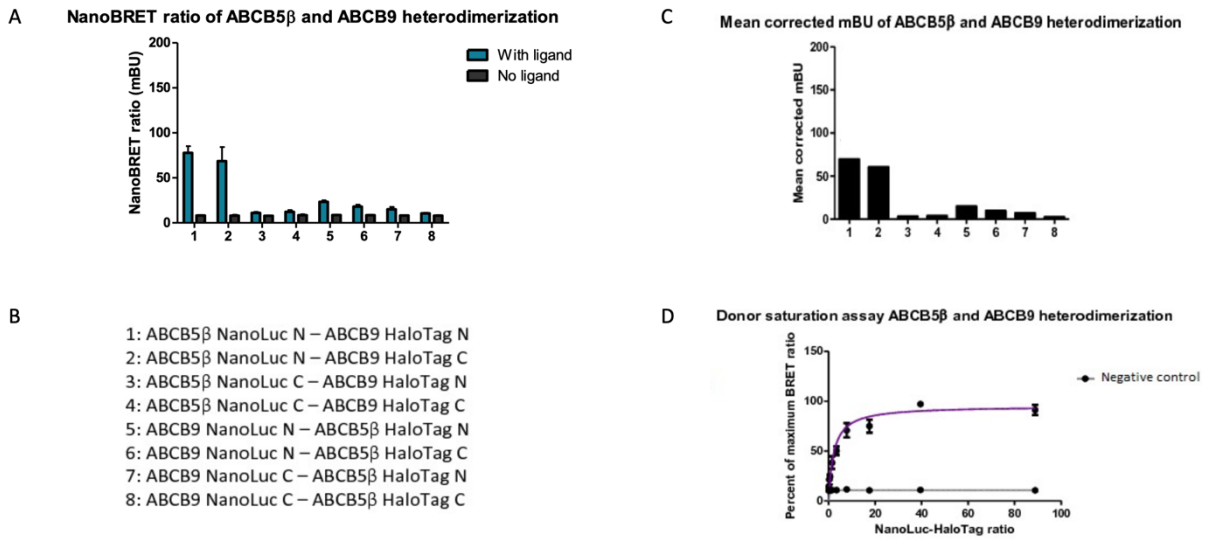

Figure 9 – Investigation of ABCB5β and ABCB9 heterodimerization. A. NanoBRET ratio obtained for each combination of ABCB5β and ABCB9 with and without ligand (negative control). **B.** All the possible combinations for ABCB5β and ABCB9 pairs by adding either NanoLuc or HaloTag in N or C terminal. **C.** Mean corrected mBU (= NanoBRET ratio without de ligand – NanoBRET ratio with the ligand) was calculated for each pair. **D.** The first pair highlight the highest NanoBRET ratio and was therefore seleceted for the donor saturation assay. The donor saturation assay for of ABCB5β and ABCB9 heterodimerization shows a saturation binding curve, meaning that it is a specific interaction. It has been done using nine different NanoLuc-HaloTag ratios. A negative control, DMSO, is added instead of the ligand. These data show a heterodimerization of ABCB5β and ABCB9.

Given that both studies, i.e. co-immunoprecipitation and NanoBRET assay, were performed using transfection of mcherry-tagged ABCB5β and ABCB9, we aimed to highlight their heterodimerization in cell lines that constitutively express both transporters.

Three different cell lines were carefully chosen for our research.

MDA-MB-231, a breast cancer cell line, was selected because, according to the cancer genome atlas database (TCGA), breast cancer represents the second cancer where ABCB9 expression is the most important.

MDA-MB-435, which highly expresses both ABCB5β and ABCB9 [29]. The MDA-MB-435 cell line was originally proposed to be derived from pleural effusion of a female breast cancer patient in 1976 at MD-Anderson (USA) [86]. Further molecular characterization revealed that these cells were actually of melanoma origin [87].

Immortalized Sertoli cells, which highly express ABCB9 [34, 39]. ABCB5β expression in these cells remains to be demonstrated. However, its expression in testis has already been shown [34].

After confirmation of both transporter expression in the selected cell lines, using RT-qPCR and western blot, the first aim of this research project was to elucidate controverted ABCB9 and ABCB5β localization using cell fractionation. The last step consisted in the validation of ABCB5β and ABCB9 heterodimerization in cells that constitutively express both transporters using co-immunoprecipitation (**Figure 10**).

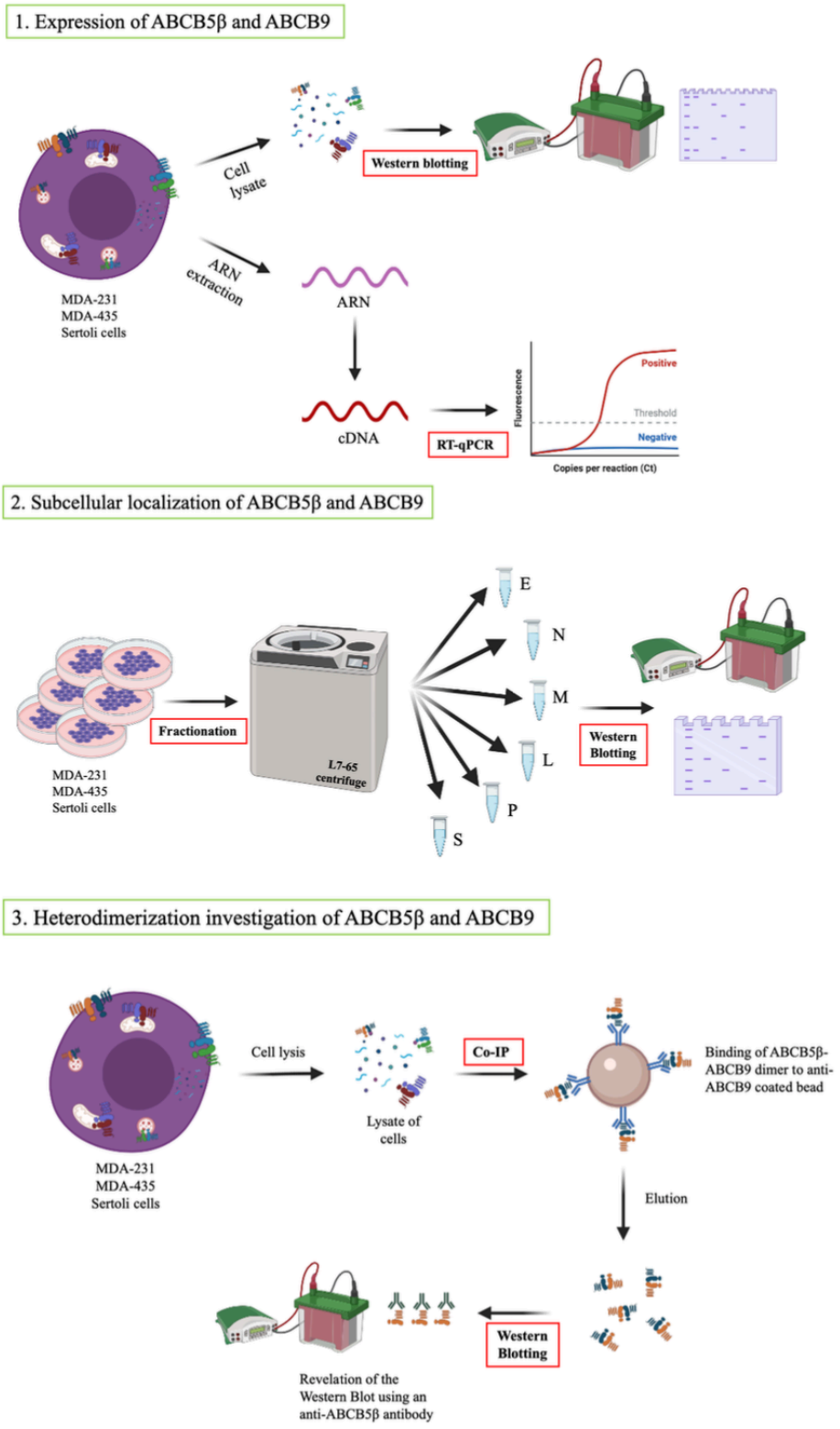

Figure 10 – Schematic overview of the investigation of ABCB5β and ABCB9 localization and heterodimerization. The first step was to check the expression of those two transporters in the three selected cell lines (MDA-MB-231; MDA-MB-435 and Sertoli cells) using western blot and RT-qPCR. The second step was to localize both transporters using cell fractionation relying on different centrifugations with increased speed to separate each organelle based on their density and size (N = nucleus, M = heavy mitochondria, L = light mitochondria and lysosomes, P = plasma membrane, ER and golgi membrane, S = soluble fraction). Last step was to study their potential heterodimerization using co-immunoprecipitation. Figure created with BioRender.com.

Unfortunately, the antibody targeting ABCB5β currently available in the lab (Rockland, Philadelphia, USA) did not allow us to detect ABCB5β expression as it lacks specificity (**Figure 11**).

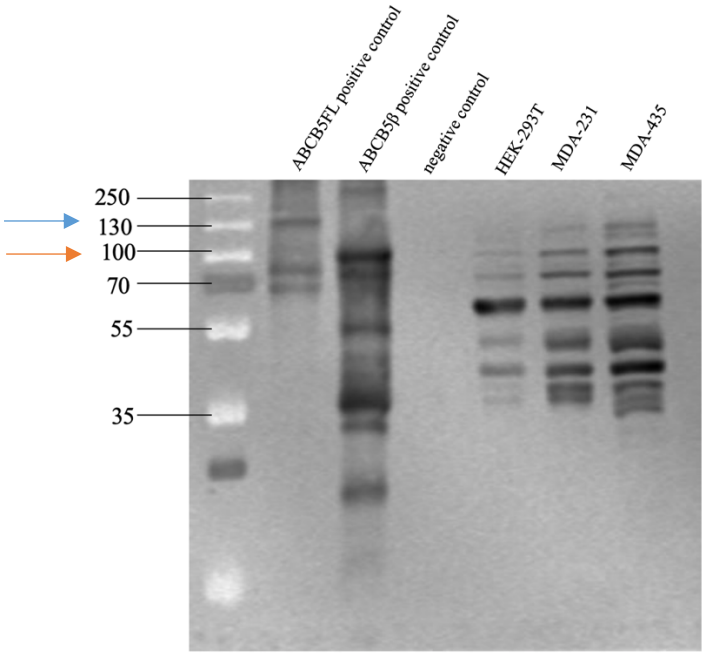

Figure 11 – Detection of ABCB5 in different cell lines. WB using anti-ABCB5 (Rockland, Philadelphia, USA) as primary antibody and anti-rabbit antibody as secondary antibody (ScanLater anti-rabbit R8204, Molecular Devices, San Jose, USA). The positive controls consist in crude membranes isolated from ABCB5 FL or ABCB5 β expressing high five insect cells and the negative control were crude membranes isolated from high five insect cells. ABCB5 FL is expected to be seen at 137 kDa (blue arrow) and ABCB5β is expected to be seen at 89 kDa (orange arrow). On this gel, multiple bands are seen for the positive control conditions, for HEK293T, MDA-MB-231 and MDA-MB-435 which makes it difficult to interpret.

Consequently, it was decided to focus on ABCB6 rather than ABCB5β based upon preliminary data in our laboratory, which suggest their possible heterodimerization. Indeed, during her master thesis, Louise Gerard also showed the dimerization of ABCB6 and ABCB9 using NanoBRET assay (**Figure 12**) [85]. ABCB9 and ABCB6 were both suspected to be localized in the lysosomes as abovementioned [41, 45, 54]. They also have an additional transmembrane domain, TMD0, which is needed for their lysosomal targeting [16, 39]. Furthermore, they both seems to have an implication in breast cancer [49, 55].

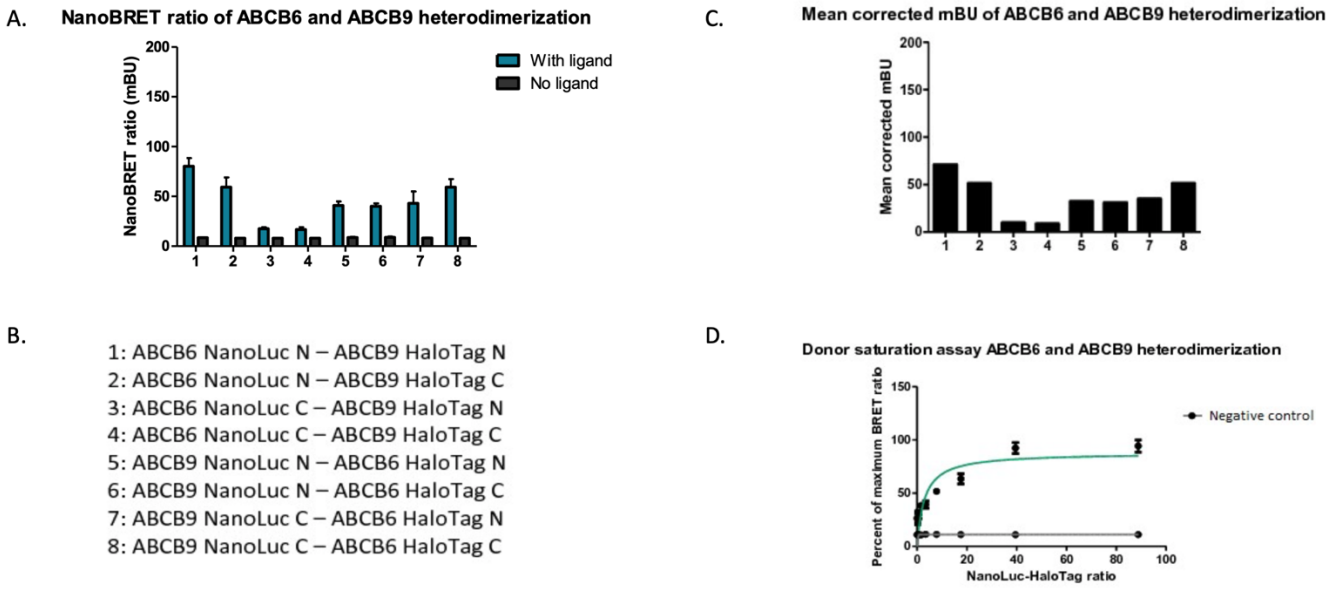

Figure 12 – Investigation of ABCB9 and ABCB6 heterodimerization. A. NanoBRET ratio obtained for each combination of ABCB9 and ABCB6 with and without ligand (negative control). **B.** All the possible combinations for ABCB9 and ABCB6 pairs by adding either NanoLuc or HaloTag in N or C terminal. **C.** Mean corrected mBU (= NanoBRET ratio without de ligand – NanoBRET ratio with the ligand) was calculated for each pair. **D.** The first pair highlight the highest NanoBRET ratio and was therefore seleceted for the donor saturation assay. The donor saturation assay for of ABCB5β and ABCB9 heterodimerization shows a saturation binding curve, meaning that it is a specific interaction. It has been done using nine different NanoLuc-HaloTag ratios. A negative control, DMSO, is added instead of the ligand. These data show a heterodimerization of ABCB9 and ABCB6 [85].

In consequence, the expression of ABCB9 and ABCB6 was investigated in the three selected cell lines (MDA-MB-231, MDA-MB-435 and Sertoli cells) by RT-qPCR and western blot. Then, their localization was analyzed using cell fractionation, and their potential heterodimerization was further investigated using co-immunoprecipitation.

3 Materials and Methods

3.1 Cell culture

MDA-MB-231 and MDA-MB-435 were cultured in Dulbecco's Modified Eagle Medium (Lonza, Basel, Switzerland) supplemented with 10% of Fetal Bovine Serum (Sigma Aldrich, Saint Louis, Missouri, USA) and 1% of penicillin (Lonza, Basel, Switzerland). Sertoli cells were cultured in PriGrow IV medium (Applied Biological Materials, Vancouver, Canada) supplemented with 10% of Fetal Bovine Serum (Sigma Aldrich, Saint Louis Missouri, USA) and 1% of penicillin (Lonza, Basel, Switzerland). Cells were maintained at 37°C 5% of CO_2.

3.2 Transfection

HEK293T, MDA-MB-231 and MDA-MB-435 were transfected with pCA-βeGFP or pcDNA3.1 B9-mCherry. 2 mL of cells were plated at $4x10^5$ cells/ml in a 6-well plate using the Vi-cell XR (Beckman Coulter, Brea, California USA). When they were between 60-80% of confluence they were transfected with 2 µg of DNA diluted in 200 µL of jetPRIME® buffer. After a quick vortex and spin down, 4 µL of jetPRIME® reagent were added to the mix, vortexed and spun down then incubated during 10 minutes at room temperature. Then, the transfection mix was added to the cells and the 6-wells plates was incubated during 48 hours at 37°C 5% CO_2 before fractionation, protein extraction or microscope observation.

3.3 Protein extraction

Cells were counted using Vi-cell XR (Beckman Coulter, Brea, California USA) to plate $4x10^5$ cells/mL on a 6-well plate. Around 90% confluence, lysis buffer (150 mM NaCl; 50 mM Tris-HCl pH 7,4; NP40 1%; 1 mM EDTA; 75 mM N-Ethylmaleimide (NEM)) with 100X protease inhibitor cocktail (PIC, Thermo scientific, Waltham, USA) was added to each well and cells were harvested using a scraper. Cells were put on a rotating wheel at 4°C for 30 minutes then centrifuged at 15 000xg during 15 minutes at 4°C. The supernatant was collected and proteins were quantified using Pierce™ BCA Protein assay kit (Thermo scientific, Waltham, USA) following manufacturer instructions.

3.4 Reverse transcriptase - quantitative polymerase chain reaction (RT-qPCR)

Cells (MDA-MB-435, MDA-MB-231, Sertoli cells) were grown in cell culture flask T75. Once they reached 90% confluence, cells were rinsed with 4 mL of PBS (Lonza, Basel, Switzerland) and trypsinized with 2 mL Trypsin EDTA (Lonza, Basel, Switzerland). Trypsin was neutralized by 8 mL of DMEM medium (Lonza, Basel, Switzerland) supplemented with 10% of Fetal Bovine Serum (Sigma Aldrich, Saint Louis, Missouri, USA) and 1% of penicillin (Lonza, Basel, Switzerland). Cells were transferred in a 15 mL tube and centrifuged during 3 minutes at 300 g. The supernatant was thrown away. The pellet was washed in 1 ml PBS and centrifuged again during 3 minutes at 300g. The supernatant was thrown away and the pellet was resuspended and homogenized in 1 mL of RiboZol® RNA Extraction Reagent (VWR Life Science, Fontenay-sous-Bois, France) in an Eppendorf. The Eppendorf was frozen during at least 1 hours at -80°C. Then, 200 µL of chloroform were added to the Eppendorf, agitated during 15 seconds by inversion and incubated for 5 minutes at room temperature. The Eppendorf was centrifuged at 13201xg during 15 minutes at 4°C. Three different phases were observed, the top one containing the RNA was collected and mixed with an equal volume of 70% ethanol. Then, RNA extraction was performed following RNeasy Mini Kit (Qiagen, Hilden, Germany) instruction. RNA yield was quantified using the SpectraMaxi3, SoftMax Pro 6.5.1 program, SpectraDrop Abs DNA RNA Quant (Molecular devices, San José, USA).

Following RNA extraction, a master mix using High capacity cDNA reverse transcription kit (Applied Biosystems, Foster city, USA) was prepared for the reverse transcription (3 µL of 10X RT buffer, 1,2 µL of dNTP Mix, 3 µL of RT random primer, 1,5 µL of multiscribe RT and 6,3 µL of Nuclease free water). The master mix and 15µl of RNA diluted to 200 ng/µL were put in PCR compatible tubes and the following cycle was performed on a C1000 Touch Thermal cycle device (BioRad, Hercules, USA), 25°C during 10 minutes, 37°C during 120 minutes, 85°C during 5 minutes and 4°C until the tubes were collected.

1 µL of cDNA was added to the master mix prepared for the quantitative PCR (8 µL TaqMan Mix, 1 µL TaqMan probes, 8 µL Nuclease free water, Applied Biosystems, Foster city, USA). The cDNA was amplified by quantitative PCR using specific TaqMan probes (**Table 4**) (Applied Biosystems, Foster City, USA) for each ABCB transporters of interest.

ABC transporter	Specific TaqMan probes reference
ABCB6	HS00180568_m1
ABCB9	HS00608634_m1
18 S	HS03003631_g1

Table 4 – Specific TaqMan probes used for the quantitative PCR

The samples were added in triplicates to a hard-shell PCR plates (Bio-Rad, Hercules, USA) and the following program was performed on a CFX96 Touch, Bio-Rad CFX Maestro program (BioRad, Hercules, USA), 50°C for 10 minutes, 95°C for 5 minutes, 95°C during 10 seconds, 60°C for 30 seconds and go to 3 (95°C 10 seconds) and 4 (60°C 30 seconds) 39 times. A reference gene to normalize the results and a negative control were used, instead of adding 1 µL of TaqMan probes of the transporter of interest, 1 µL of 18S TaqMan probe was added and for the negative control, 1 µL of water was added.

3.5 Subcellular fractionation

Cells were grown in 6 petri dishes (0.55 dm^2) until they reached 90% of confluence. The dishes were placed on ice and washed three times with cold isotonic sucrose 0.25 M. In each petri dish, cells were scraped with 0.5 mL of sucrose and transferred in a 7 mL Dounce (Sigma-Aldrich, Saint Louis, USA). Cells were homogenized with 30 passages for MDA-MB-231 and 15 passages for MDA-MB-435. The homogenate (H) was fractionated with successive centrifugation pelleting at 4°C described below. In a 15 mL tube, volume was adjusted to 4 mL with sucrose 0.25 M and H was centrifuged in Allegra X-30R Centrifuge (Beckman Coulter, Brea, USA) rotor SX4400 for 8 minutes at 1000 x g. After collection of the supernatant 0.5 cm above the pellet, the pellet (Fraction N) was resuspended and homogenized in a Dounce with the same number of passages previously used. The volume was adjusted to 2 mL with sucrose 0.25 M and N was centrifuged for 7 minutes 32 seconds at 1000 x g. Both supernatants (E fraction) were centrifuged in a L7-65 centrifuge (Beckman Coulter, Brea, USA) rotor 75.1 Ti. For all following centrifugation, time were defined depending on the volume in the tube (**Appendix 1**). Each centrifugation was performed a second time after collection of the supernatant to wash the pellet, except for P fraction. Centrifugation speed were the following, 8000 rpm (Fraction M), 25000 rpm (Fraction L), 35 000 rpm (Fraction P). The remaining supernatant corresponded to the fraction S. To collect the supernatant maximal decantation were applied, except for the pellet M, where a minimal decantation was performed. Each fraction was weighted to determine the dilution performed based on the E fraction (containing M, L, P, S) and the surface of the petri dishes.

Each fraction is analyzed using western blotting. Different primary antibodies were used; anti-ABCB9 (Santa Cruz biotechnology, Dallas, USA), anti-ABCB6 (Santa Cruz biotechnology,

Dallas, USA), anti-TOMM20 (Santa Cruz biotechnology, Dallas, USA) and anti-histone H1 (Abcam, Cambridge, UK). Secondary antibodies were used as described in the 3.6 section.

3.5.1 Protein dosage and enzyme assays

Protein levels were measured using Pierce BCA Protein Assay Kit (Thermo Scientific, Massachusetts, USA), following manufacturer's instructions.

The enzymatic activity of the following enzymes, alkaline α-glucosidase, β-hexosaminidase and alkaline phosphodiesterase was evaluated after fractionation.

For alkaline α-glucosidase, 4-Methylumbelliferone (4MU)-α-D-glucopyranoside (Sigma-Aldrich, Saint-Louis, USA) was diluted in DMSO to obtain a concentration of 10 mM. Then 300 µL of diluted substrate was added to 600 µL glycine 0.5M – NaOH pH9, 2,1 mL of water and 6 µL of triton X-100 20%. Each fraction obtained during the fractionation was diluted as follows:

- E-N-M-L-S : ½ and ¼
- P : ¼ and 1/8

Each fraction was incubated with 90 µL of the final mix in polystyrene cuvettes (Sarstedt, Nümbrecht, Germany) at 37°C during 4 hours. The reaction was stopped by addition of 1 mL of 0.1M glycine buffer pH 10. Fluorescence was read at 495nm using VersaFluor (Bio-Rad, Hercules, US).

To assess β-hexosaminidase activity, 4-MU-N-acetyl-β-D-glucosaminide (Sigma-Aldrich, Saint-Louis, USA) was diluted in DMSO to obtain a concentration of 50 mM. Then, 130 µL of diluted substrate was diluted with 1,17 mL of 50 mM citrate + 0.05% triton buffer pH 4.5 to obtain a final concentration of 5 mM. Each fraction obtained during the fractionation was diluted as follows:

- E-N-P-S : ½ and ¼
- M-L : ¼ and 1/8

Each fraction was incubated with 90 µL of the final mix in polystyrene cuvettes (67.754, Sarstedt, Nümbrecht, Germany) at 37°C during 1 hours. The reaction was stopped by addition of 1 mL of 0.1M glycine buffer pH 10. Fluorescence was read at 495nm using VersaFluor (Bio-Rad, Hercules, US).

To assay the alkaline phosphodiesterase, thymidine 5' monophosphate p-nitrophenyl ester sodium salt (Sigma-Aldrich, Saint-Louis, USA) was diluted in 1 mL of glycine 0.5M adjusted with NaOH pH 9.6, 1 mL of zinc acetate 0.01M, 60 µL NaOH 1M and 2,54 mL of water to obtain a concentration of 1,5 mM. Each fraction obtained during the fractionation was diluted as follows:

- E-M-L : ½ and ¼
- N-P : 1/5 and 1/10
- S : no dilution

Each fraction was incubated with 115 µL of the final mix in polystyrene cuvettes (67.742, Sarstedt, Nümbrecht, Germany) at 37°C until a strong yellow coloration appears. The reaction was stopped by addition of 1 mL of 0.1M glycine buffer pH 10. Fluorescence was read at 400nm using Genesys 50 UV-visible Spectrophotometer (Thermo Fisher Scientific, Massachussetts, USA).

To assay the dipeptidyl peptidase III, 536 H-Arg-Arg-AMC hydrochloride salt (Bachem holding, Bubendorf, Switzerland) was diluted in DMSO to obtain a concentration of 0,25 mM. Then 13,3 µL of the mix was diluted in 333 µL of TRIS-Cl 0,5M pH8 and 653 µL of water. 10 µL of each fraction obtained during the fractionation was incubated with 90 µL of the final mix in polystyrene cuvettes (67.742, Sarstedt, Nümbrecht, Germany) at 37°C during 1 hour. The reaction was stopped by addition of 1,2 mL of 50 mM glycine/EDTA 5 mM/TritonX-100 0,05% pH10,5. Fluorescence was read at 495nm using VersaFluor (Bio-Rad, Hercules, US).

3.6 Co-immunoprecipitation

50 µg of proteins were diluted in 200 µL of lysis buffer (150 mM NaCl; 50 mM Tris-HCl pH 7,4; NP40 1%; 1 mM EDTA; 75 mM N-Ethylmaleimide (NEM)). 1 µg of antibody, either anti-ABCB6 (Santa Cruz biotechnology, Dallas, USA) or anti-ABCB9 (Santa Cruz biotechnology, Dallas, USA), was added to the protein. A negative control was done by adding 1 µg of IgG (Santa Cruz biotechnology, Dallas, USA) instead of an anti-ABC antibody. Samples were incubated on a rotating wheel during 4 hours at 4°C. During the incubation, 25 µL of magnetic beads *Dynabeads-Protein G* (Invitrogen, Carlsbad, USA) and 25 µL of *Dynabeads-Protein A* (Invitrogen, Carlsbad, USA) were washed two times with 250 µL of lysis buffer on a magnetic rack. Once the incubation was over, samples containing antibody and proteins were added to the magnetic beads and incubated overnight on a rotating wheel at 4°C. On the next day, the beads were washed three times with 250 µL of cold PBS + 0,5% Tween 20. Proteins were eluted with 50 µL of loading buffer at 40°C during 10 minutes. The supernatant was collected and put on a western blot to asses protein expression (either with anti-ABCB6 or anti-ABCB9 depending on the antibody used to precipitate).

3.7 Western Blot (WB)

Proteins (5 µg for expression WB, 10 µg for fractionation WB, 50 µg for Co-Ip) were loaded on an 8% SDS-acrylamide gel and migrated at 90 V. Then they were transferred to a PVDF membrane (BioRad, Hercules, USA) at 110 V during 1h30. The membrane was blocked with 5% milk PBS Tween 20 0,5% during 1 hour and then incubated overnight at 4°C with the primary antibody (**Table 5**) diluted in the blocking buffer. The day after, the membrane was washed three times in PBS + 0,5% Tween 20 during five minutes. Afterwards, the membrane was incubated with the secondary antibody, either anti-rabbit (#R8202, ScanLater, Molecular Devices, California, USA) or anti-mouse (#R8201, ScanLater, Molecular Devices, California, USA) depending on the primary antibody used, for one hour. Membrane was washed three times with PBS Tween 20 0,5% for 5 minutes and rinsed with distilled water for 15 seconds. Membranes were revealed with the SpectraMax SoftMax Pro 6.5.1 program, (Molecular devices, San José, USA). If a fluorescent secondary antibody were used, IRDye 800CW donkey anti-goat (LI-COR, Lincoln, Nebraska, USA), two washes of 20 minutes in PBS Tween 20 0,5% followed with one wash in PBS during 20 minutes were performed. The revelation was done with the LI-COR Odyssey (LI-COR biosciences, Lincoln, US).

Primary antibody	Dilution	Reference
ABCB6 (Anti-Mouse)	1/200	Santa Cruz biotechnology, Dallas, USA
ABCB9 (Anti-Mouse)	1/200	Santa Cruz biotechnology, Dallas, USA
TOM20 (Anti-Mouse)	1/500	Santa Cruz biotechnology, Dallas, USA
Histone H1 (Anti-rabbit)	1/1000	Abcam, Cambridge, UK
Tomato (mCherry) (Anti-goat)	1/1000	Sicgen, Cantanhede, Portugal
Alpha-tubuline	1/200	Abcam, Cambridge, UK

Table 5 – Primary antibodies and their dilution used during western blot

3.8 shRNA transfection

HEK293T cells were plated in 6 well-plates, $2x10^5$ cells per mL. They were grown during 24h to a 50% confluency in antibiotic-free DMEM supplemented with 10% FBS. ABCB9 shRNA plasmid (Santa Cruz biotechnology, Dallas, USA) was transfected using the manufacturer instruction (Santa Cruz biotechnology, Dallas, USA). The following specific conditions were applied: two different ratio of shRNA plasmid DNA: shRNA plasmid transfection reagent was used, 1:1 and 1:4. The shRNA DNA and transfection reagent were incubated for 30 minutes before adding them to the cells. The transfected cells were incubated for 7 hours at 37°C 5% CO_2 before the addition of 2 times normal growth medium (DMEM supplemented with 2% Penicillin/Streptomycin and 20% FBS, Lonza, Basel, Switzerland). Then, the cells were incubated for an additional 24 hours at 37°C 5% CO_2. Finally, protein and RNA were harvested as explained in section 3.3 and 3.4 and western blot and RT-qPCR were performed as section 3.7 and 3.4.

4 Results

4.1 Protein and mRNA expression of ABCB9 and ABCB6 in MDA-MB-231, MDA-MB-435 and Sertoli cell lines

The first step of this project was to confirm experimentally that the three cell lines constitutively express ABCB9 and ABCB6. Therefore, their protein expression was investigated using western blot and their mRNA expression using RT-qPCR in the three chosen cell lines; MDA-MB-231, MDA-MB-435 and Sertoli cells. Regarding protein expression, cells were lysed and proteins were extracted. Five µg of proteins were loaded on a gel and the expression of ABCB9 (**Figure 13A**) and ABCB6 (**Figure 13B**) was analyzed. The molecular weights of ABCB9 and ABCB6 are 84 kDa and 79 kDa, respectively.

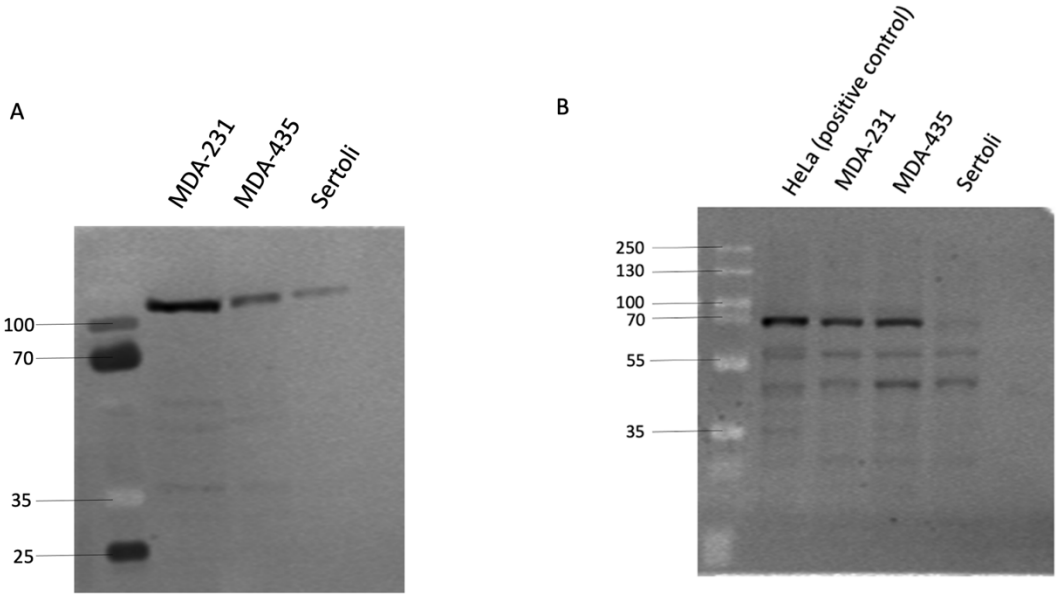

Figure 13 – Western blot to analyze protein expression of ABCB9 (A) and ABCB6 (B) in MDA-MB-231, MDA-MB-435 and Sertoli cells. (A) Each cell line was lysed and proteins harvested were used to perform a western blot, revelation of ABCB9 was done using anti-ABCB9 (Santa Cruz biotechnology, Dallas, USA). A band at 84 kDa is expected if the cell lines express the ABCB9 transporter (B) Each cell line was lysed and protein harvested were used to performed a western blot, revelation of ABCB6 was done using anti-ABCB6 (Santa Cruz biotechnology, Dallas, USA). A band at 79 kDa is expected if the cell line express ABCB6 transporter. HeLa cells were used as a positive control for the expression of ABCB6.

The western blot for ABCB9 (**Figure 13A**) shows a band for each cell lines, which is found to be above 100 kDa. This may correspond to ABCB9 after post-translational modifications, like glycosylation of the protein. For the ABCB6 blot, bands are observed near 70 kDa in the positive control, the MDA-MB-231 and MDA-MB-435 cell lines, but not in the Sertoli cell line. HeLa cell line was used as the positive control for ABCB6 because it is the control suggested by the antibody manufacturer (Santa Cruz Biotechnology, Dallas, USA). HEK293T cells should have been used as the positive control for ABCB9 as per the manufacturer recommendation (Santa Cruz Biotechnology, Dallas, USA) [17].

For the mRNA expression, cells were lysed then RNA was extracted for each cell line and converted into cDNA using reverse transcriptase. 1 µg of cDNA of each cell lines was mixed with specific probe of either ABCB6 or ABCB9 and the quantitative PCR was performed (**Table 6**).

ABCB6	Mean Ct (SD)	Mean 18S Ct (SD)	ΔCt	Mean ct H2O (-ctrl)
MDA-MB-231	28,3 (0,17)	10,9 (0,17)	17,4	N/A
MDA-MB-435	26,2 (0,12)	10,4 (0,15)	15,8	N/A
Sertoli cells	25,5 (0,14)	9,18 (0,24)	16,3	N/A
ABCB9	**Mean Ct (SD)**	**Mean 18 Ct (SD)**	**ΔCt**	**Mean ct H2O (-ctrl)**
MDA-MB-231	29,2 (0,02)	10,9 (0,17)	18,3	38,8
MDA-MB-435	29,8 (0,02)	10,4 (0,15)	19,4	38,8
Sertoli cells	29,4 (0,12)	9,18 (0,24)	20,2	38,8

Table 6 – RT-qPCR performed to detect mRNA expression of ABCB9 and ABCB6 in MDA-MB-231, MDA-MB-435 and Sertoli cells. Ct represents the number of cycles at which the fluorescence level is above the background fluorescence (threshold). 18S ribosomal RNA was used as a housekeeping gene. The mean Ct was measured from three biological replicates. The ΔCt is the Mean Ct – Mean 18 Ct. Water is used as a blank; its mean Ct is N/A and 38,8 for ABCB6 and ABCB9, respectively.

Concerning the RT-qPCR, the mean Ct values for ABCB6 probes are 28,3, 26,2 and 25,5 for MDA-MB-231, MDA-MB-435 and Sertoli cell lines, respectively. For ABCB9 probes, the mean Ct values are 29,2, 29,8 and 29,4 for MDA-MB-231, MDA-MB-435 and Sertoli cell lines, respectively. These data reveal that each cell lines express ABCB9 and ABCB6 at the mRNA level. 18S is used as a housekeeping gene because it has a consistent expression across tissues and cells [88].

In summary, ABCB6 and ABCB9 mRNA expression was identified in each selected cell lines. At the protein level, both transporters were identified in the MDA-MB-231 and MDA-MB-435 cell lines. However, ABCB6 protein was not detected in the Sertoli cell line.

4.2 Subcellular localization of ABCB9 and ABCB6 in MDA-MB-231 and MDA-MB-435 cell lines

After verification of ABCB9 and ABCB6 expression in each cell line, we pursued our project using MDA-MB-231 and MDA-MB-435 cell lines since they express both transporters at the protein level. Both transporter localization is under debate in the literature. Therefore, we needed to assess in which organelles they were expressed. To do so, subcellular fractionation was used. It consists in successive centrifugation steps based on differential sedimentation after homogenization of the cells in sucrose 0,25 M. This technique relies on the different coefficient of sedimentation of the subcellular compartments to isolate them from one another. This coefficient takes into account the size and density of organelles. The largest ones sediment faster at lower velocities and the smallest ones take longer at higher velocities. Successive centrifugation of homogenized cell extract was done, with increasing centrifugal forces, which allows to sediment organelles with different sedimental forces.

Five subcellular fractions are obtained using the differential centrifugation described by de Duve [89]. The N fraction is the nuclear fraction. The M fraction is the heavy mitochondrial fraction, whereas the L fraction is the light mitochondrial fraction. The L fraction is less abundant in lysosomes but has a higher enrichment factor due to the presence of fewer mitochondria. The P fraction is the microsomal one where ER, golgi and plasma membrane fragments are enriched after being broken down into small vesicles (microsomes). And finally, S is the cytosolic soluble fraction.

Following fractionation, several enzymatic dosages are performed to make sure that the enrichment of each organelles is in the corresponding fraction. To do so, the distribution profile of four enzymes and two protein markers were used; histone H1 (nucleus), TOM21 (mitochondria), beta-hexosaminidase (lysosome), alpha-glucosidase (endoplasmic reticulum), alkaline phosphodiesterase (plasma membrane) and dipeptidyl peptidase III (cytoplasm). Each distribution profile is represented in **Figure 14** for MDA-MB-231 and **Figure 16** for MDA-MB-435.

The alpha-glucosidase is a specific ER enzyme, therefore it is expected to be in the P fraction where the majority of microsomes are. The beta-hexosaminidase is a lysosomal peptidoglycan hydrolase. As lysosomes mainly sediment in the L fraction, this enzyme is expected to be in this L fraction. The alkaline phosphodiesterase is a plasma membrane enzyme, comparably to the ER, it is expected to be found in the P fraction. The dipeptidyl peptidase III is a soluble enzyme found in the S fraction.

Each graph for the enzymatic distribution profile has on the x-axis the percentage of proteins in each fraction. The Specific Relative Activity (SRA), which is the value obtained when the % of activity in the fraction is divided by the % of proteins in this fraction, is represented on the y-axis. Thus, the SRA is a representation of the relative enzyme enrichment in the fraction. To summarize, each fraction is represented by a rectangle whose surface reflects the relative activity of the enzyme within a fraction.

Anti-histone H1 and anti-TOM20 were used as nuclear and mitochondrial markers, respectively, to assess the distribution profile of the N and M fractions. The markers were detected by western blot and quantified using ImageJ software to obtain their distribution profile.

Image J (National Institutes of Health, version 1.53) is a software that allows the quantification of western blot. It was used to quantify Histone H1, TOM20, ABCB9 and ABCB6 signals in each fraction. The signal observed in each fraction and quantified by ImageJ is used in this formula:

$$\text{Relative specific signal (RSS)} = \frac{100}{\Sigma \text{ total WB signal in each fraction} \div \text{total signal within a specific fraction}}$$

The relative specific signal (RSS) is the percentage of proteins of interest in a specific fraction divided by the percentage of proteins in the same fraction. In summary, the graph (**Figure 14E-F and 16E-F**) shows each fraction which is represented by a rectangle whose surface reflects the relative amount of the protein of interest in the fraction.

4.2.1 ABCB9 and ABCB6 localization in MDA-MB-231 cell line by subcellular fractionation

For MDA-MB-231 fractionation, the enzymatic dosage and markers quantification are presented in **Figure 14**. Six petri dishes were used and 30 passages were performed. TOM20 and Histone H1 were detected by western blot, where 10 µg of each fractions were loaded on a SDS-page gel and revealed either with anti-histone H1 (Abcam, Cambridge, UK) or anti-TOM20 antibody (Santa Cruz Biotechnology, Dallas, USA) as primary antibodies and anti-mouse antibody (#R8201, ScanLater, Molecular Devices, California, USA) as the secondary antibody. Their molecular weights are 26-34 kDa and 20 kDA for histone H1 and TOM20, respectively.

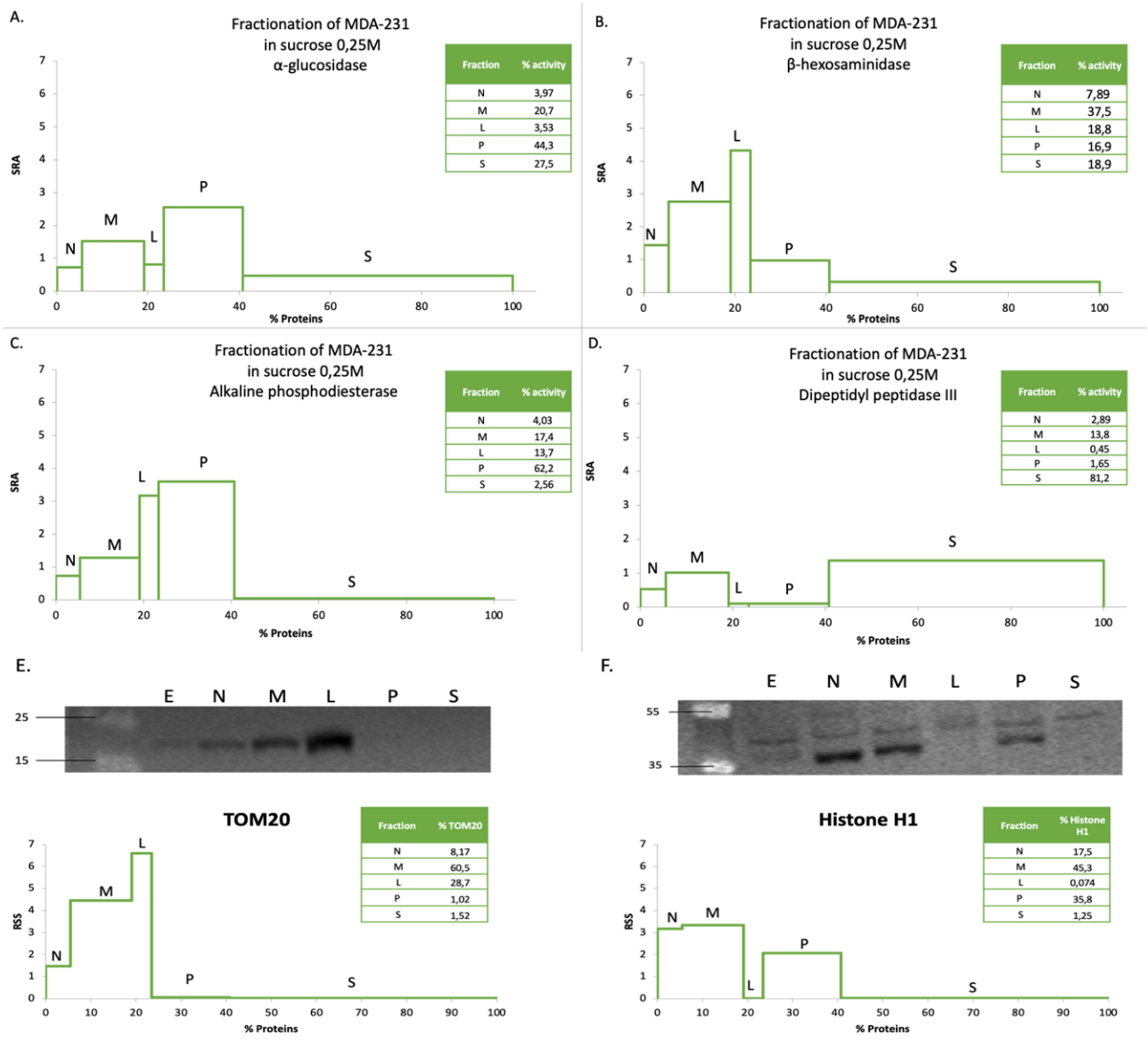

Figure 14 – Detection of the α-glucosidase, β-hexosaminidase, alkaline phosphodiesterase and dipeptidyl peptidase III enzymes, Histone H1 and TOM20 in MDA-MB-231 cell line after subcellular fractionation. MDA-MB-231 were plated in 6 petri dishes and 30 passages were performed following C. de Duve method [89]. The fractionation resulted in 5 fractions (N, M, L, P, S). Several enzymatic dosages and western blotting quantification were done to obtain distribution profiles. Enzymatic activity of **A.** α-glucosidase (endoplasmic reticulum) **B.** β-hexosaminidase (lysosome) **C**. Alkaline phosphodiesterase (plasma membrane) and **D.** Dipeptidyl peptidase III (cytosol) were measured as described in section 3.5.1. Distribution profile for **E.** TOM20 and **F.** Histone H1 were obtained by western blotting and quantified using ImageJ. 10 µg of each fraction were loaded on the blot and revealed with anti-histone H1 (Abcam, Cambridge, UK) or anti-TOM20 antibody (Santa Cruz Biotechnology, Dallas, USA) as primary antibodies and anti-mouse antibody (#R8201, Later, Molecular Devices, California, USA) as the secondary antibody. For TOM20, bands are seen at 20 kDa and for Histone H1, a band is observed at 36 kDa. The graph shows on the x-axis the % of proteins within a fraction and on the y-axis, the specific relative activity (SRA) for the enzyme and the relative specific signal (RSS) for TOM20 and Histone H1. The surface of each rectangle is the percentage of the activity/signal of the enzyme/marker within a specific fraction.

On **Figure 14**, we observe that 44,3% of the α-glucosidase is recovered in fraction P. According to the SRA, there is a high enrichment of the enzyme in fraction P. Approximately 60% of β-hexosaminidase is recovered in fractions M+L and there is a high enrichment in the L and M fraction. The alkaline phosphodiesterase is mainly found in the P fraction (62,22%) and there

is a high enrichment in fraction L and P. Finally, for the dipeptidyl peptidase III, most of the enzyme is recovered in the S fraction (81,19%) and there is a high enrichment in the S and M fractions.

Regarding the organelle markers, TOM20 is mostly in the fraction M (60,5%) as expected, there is a high enrichment in the fractions M and L. For histone H1, surprisingly it is found mostly in fractions M (45,3%) and P (35,8%) and a small percentage in the N fraction (17,5%) where it is supposed to be found. The enrichment is similar in the N and M fractions.

As each enzyme and protein markers were retrieved in the corresponded fraction (except for the Histone H1), we could move on with the analysis of the distribution of B6 and B9 in each fraction (**Figure 15**). To do so, 10 µg of each fraction were loaded on a western blot which was revealed with anti-ABCB9 (Santa Cruz Biotechnology, Dallas, USA) or anti-ABCB6 antibody (Santa Cruz Biotechnology, Dallas, USA) as primary antibodies and anti-mouse antibody (#R8201, ScanLater, Molecular Devices, California, USA) as the secondary one.

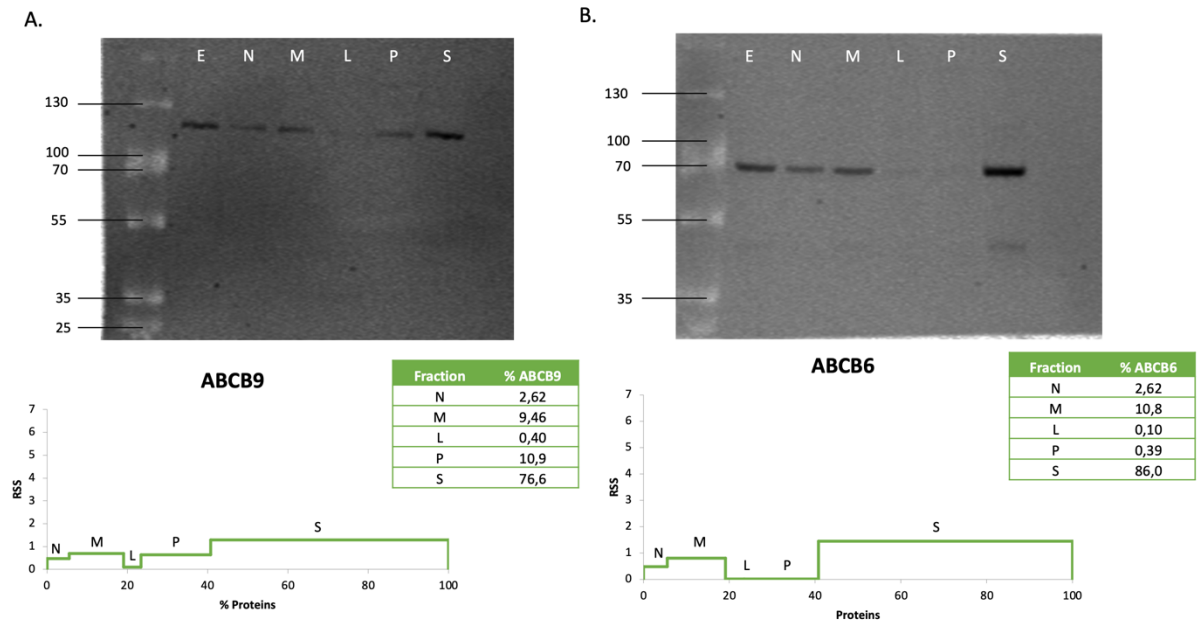

Figure 15 – Detection of ABCB6 and ABCB9 in MDA-MB-231 subcellular fractions prepared by differential centrifugation. MDA-MB-231 cells were plated in 6 petri dishes and fractionated in 5 fractions (N, M, L, P, S) following C. de Duve protocol. 10 µg of each fraction were loaded on the western blot and revealed with anti-ABCB9 (Santa Cruz biotechnology, Dallas, USA) or anti-ABCB6 antibody (Santa Cruz biotechnology, Dallas, USA) as primary antibody and anti-mouse antibody (#R8201, ScanLater, Molecular Devices, California, USA) as the secondary one. The percentage of ABCB9 and ABCB6 were calculated using Image J 1.53 software. The relative specific signal (RSS) plotted on the y-axis, represents the signal of ABCB9 or ABCB6 detected in a fraction divided by the percentage of proteins in the same fraction. ABCB9 band is expected at 84 kDA and ABCB6 band is expected at 79 kDa.

Regarding the **Figure 15**, we observe a recovery of ABCB9 mainly in the S fraction (76,6%) and an enrichment of it in the M, P and S fractions. For ABCB6, the recovery is almost entirely in the S fraction (86,0%) and there is a high enrichment in the S and M fractions. According to those results, both transporters are localized in the cytosolic fraction.

4.2.2 ABCB9 and ABCB6 localization in MDA-MB-435 cell line by subcellular fractionation

The same process as with MDA-MB-231 subcellular fractionation analysis was done for the MDA-MB-435. Several enzymatic dosages are performed to make sure that the enrichment of each organelles is in the corresponding fraction (**Figure 16**).

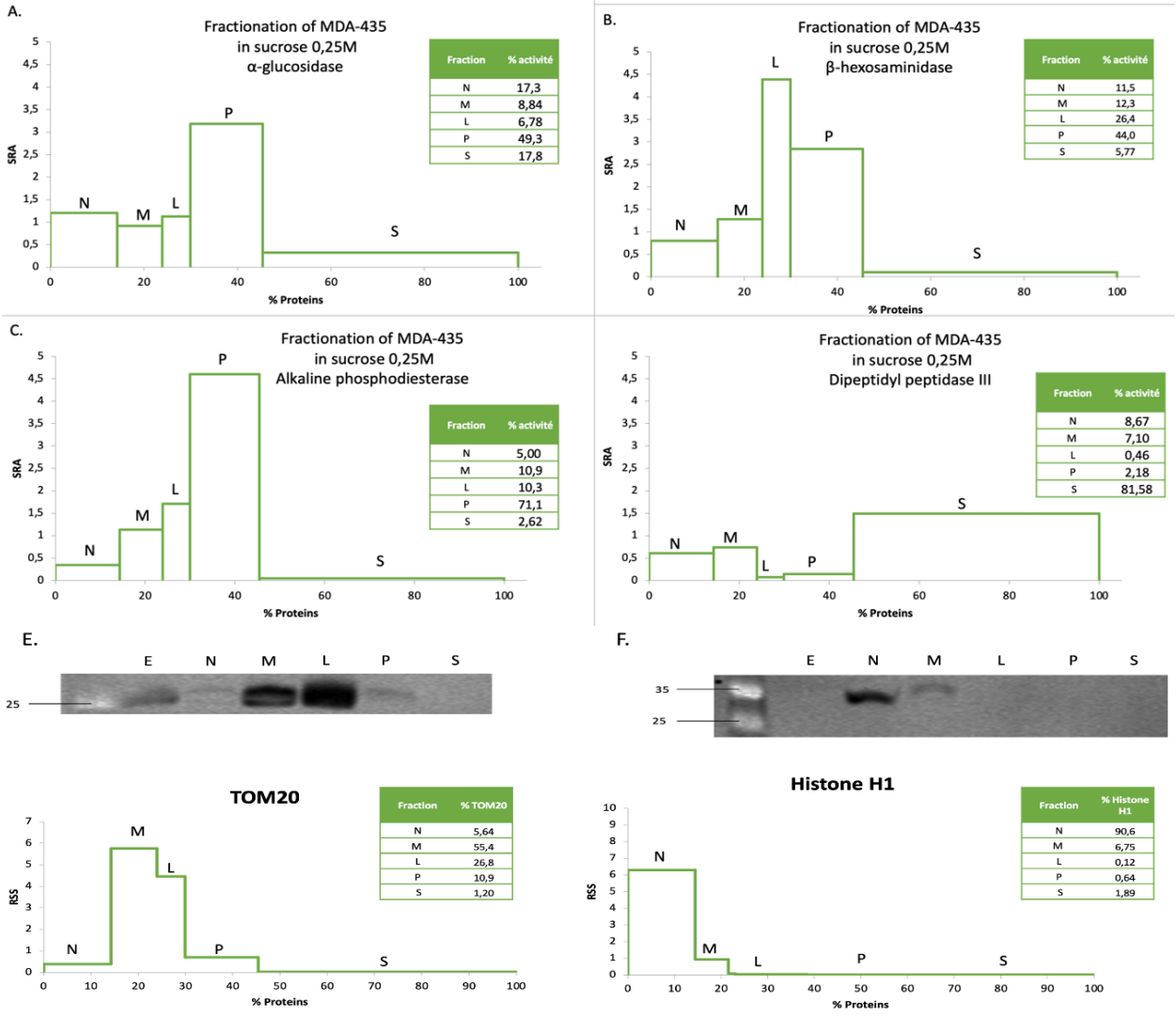

Figure 16 - Detection of the α-glucosidase, β-hexosaminidase, alkaline phosphodiesterase and dipeptidyl peptidase III enzymes, Histone H1 and TOM20 in MDA-MB-435 after subcellular fractionation. MDA-MB-435 cells were plated in 5 petri dishes and 15 passages were performed following C. de Duve method [89]. The fractionation resulted in 5 fractions (N, M, L, P, S). Several enzymatic dosages and western blotting quantification were done to obtain distribution profiles. Enzymatic activity of **A.** α-glucosidase (endoplasmic reticulum) **B.** β-hexosaminidase (lysosome) **C**. Alkaline phosphodiesterase (plasma membrane) and **D.** Dipeptidyl peptidase III (cytosol) were measured as described in section 3.5.1. Distribution profile for **E.** TOM20 and **F.** Histone H1 were obtained by western blotting and quantified using ImageJ. 10 µg of each fraction were loaded on the blot and revealed with anti-histone H1 (Abcam, Cambridge, UK) or anti-TOM20 antibody (Santa Cruz biotechnology, Dallas, USA) as primary antibodies and anti-mouse antibody (#R8201, ScanLater, Molecular Devices, California, USA) as the secondary antibody. For TOM20, bands are seen at 20 kDa and for Histone H1, a band is observed at 36 kDa. The graph shows on the x-axis the % of proteins within a fraction and on the y-axis, the specific relative activity (SRA) for the enzyme and the relative specific signal (RSS) for TOM20 and Histone H1. The surface of each rectangle is the percentage of the activity/signal of the enzyme/marker within a specific fraction.

On **Figure 16**, we observe that 49,3% of the α-glucosidase is recovered in fraction P. Approximately 70% of β-hexosaminidase is recovered in fractions M+L and there is a high enrichment in the L and P fractions. The alkaline phosphodiesterase is mainly found in the P fraction (71,1%) and there is a high enrichment in fraction P. Finally, for the dipeptidyl peptidase III, most of the enzyme is recovered in the S fraction (81,6%).

Regarding mitochondrial marker, TOM20, it is recovered at 55,4% in the M fraction and a high enrichment is found in the fractions M and L. For the nuclear marker, histone H1 is almost totally recovered and highly enriched in the N fraction (90,6%) as expected.

Once all the enzymatic dosage and western blot analysis and quantification were done, ABCB9 and ABCB6 recovery and enrichment were analyzed by western blotting. Image J was used to quantify the relative specific signal and the % of proteins of interest. On **Figure 17**, 10 µg of each fraction were loaded on the blot which was revealed with anti-ABCB9 (Santa Cruz biotechnology, Dallas, USA) or anti-ABCB6 antibody (Santa Cruz biotechnology, Dallas, USA) as primary antibodies and anti-mouse antibody (#R8201, ScanLater, Molecular Devices, California, USA) as the secondary one.

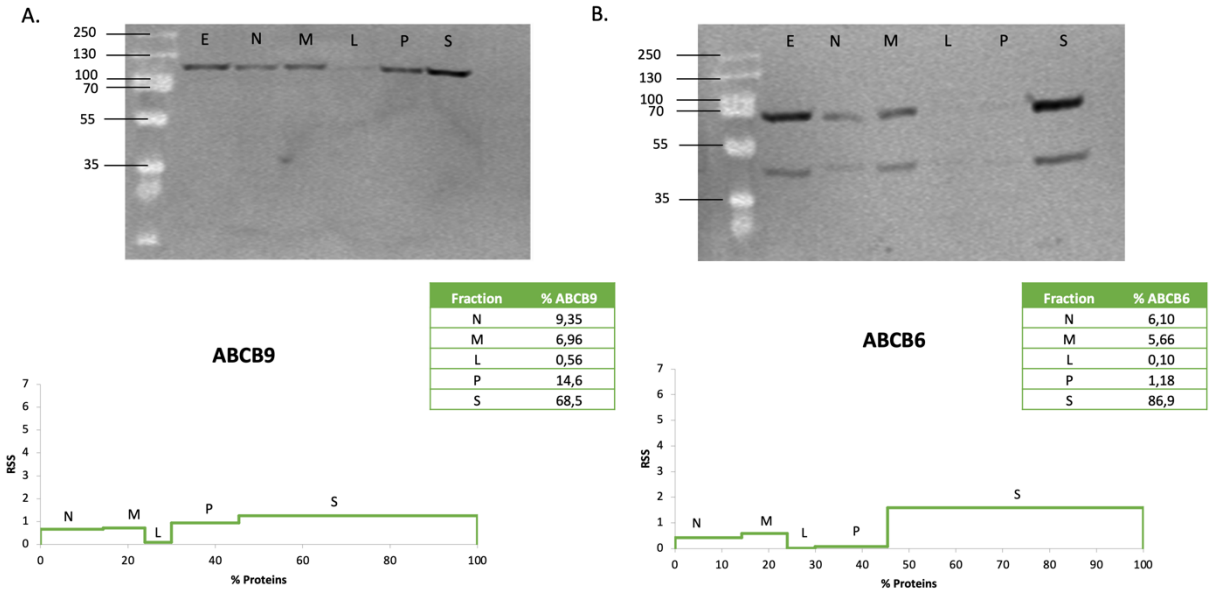

Figure 17 – Detection of ABCB6 and ABCB9 in MDA-MB-435 subcellular fractions prepared by differential centrifugation. MDA-MB-435 cells were plated in 5 petri dishes and fractionated in 5 fractions (N, M, L, P, S) following C. de Duve protocol. 10 µg of each fraction were loaded on the blot and revealed with anti-ABCB9 (Santa Cruz biotechnology, Dallas, USA) (**Figure 19A**) or anti-ABCB6 antibody (Santa Cruz biotechnology, Dallas, USA) (**Figure 19B**) as primary antibodies and anti-mouse antibody (#R8201, ScanLater, Molecular Devices, California, USA) as the secondary one. The percentage of ABCB9 and ABCB6 were calculated using Image J software. The relative specific signal (RSS) plotted on the y-axis, represents the percentage of ABCB9 or ABCB6 detected in a fraction divided by the percentage of proteins in the same fraction. 68,5% of ABCB9 is found in S fraction and 86,9% of ABCB6 is also found in S fraction. ABCB9 band is expected at 84 kDA and ABCB6 band is expected at 79 kDa.

As we can see on **Figure 17**, the fractionation of MDA-MB-435 cells showed that ABCB9 and ABCB6 are mainly found in fraction S, with 68,5% and 86,9% respectively. However, for ABCB9, we can see that the RSS is similar for fractions N, M, P and S (around 1) and for ABCB6, the enrichment is higher in the S fraction.

4.2.3 Additional investigation about the localization of ABCB6 and ABCB9

After the subcellular fractionation of MDA-MB-231 and MDA-MB-435 cell lines, ABCB6 and ABCB9 were found to be enriched and recovered in the S fraction (**Figures 15 and 17**). As both proteins are transmembrane proteins, their expression in the cytoplasm is not expected and therefore complementary experiments on the S fraction were made. It was decided to perform an additional centrifugation of the fraction S from both fractionation (i.e MDA-MB-231, and MDA-MB-435 cell lines) to investigate the possibility that microsomes had reached the S fraction (**Figure 18**). This centrifugation was done at 245 070xg during 50 minutes in the Optima TLX ultracentrifuge using TLA-120.2 rotor with 250 µL of S fraction. After the centrifugation, we obtained a supernatant and a pellet where the microsomes are suspected to be. 15 µL of the S fraction, 15 µL of the supernatant and 15 µL of the pellet resuspended in 0.25M sucrose were loaded on the gel, which was revealed with anti-ABCB9 (Santa Cruz biotechnology, Dallas, USA) or anti-ABCB6 antibody (Santa Cruz Biotechnology, Dallas, USA) as primary antibodies and anti-mouse antibody (#R8201, ScanLater, Molecular Devices, California, USA) as the secondary one. If ABCB9 or ABCB6 are indeed in the microsomes, bands should be observed at 84 kDa for ABCB9 and 79 kDa for ABCB6, only in the S fraction and in the pellet. It must be noted that during the additional centrifugation for MDA-MB-435 cells, a very small pellet, almost indistinguishable, was obtained.

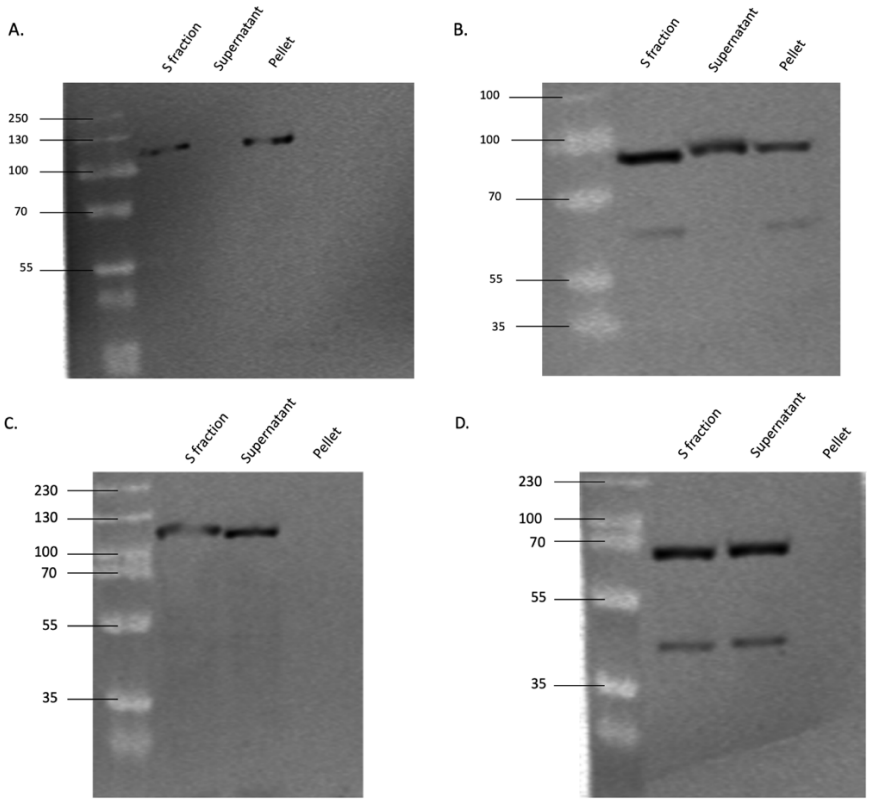

Figure 18 – Additional centrifugation of the S fraction at 245 070xg during 50 minutes in the Optima TLX centrifuge. After centrifugation, a pellet is observed and resuspended in 0,25M sucrose. 15 µL of the S fraction, 15 µL of the supernatant and 15 µL of the pellet resuspended in 0.25M sucrose were loaded on the gel, which was revealed with anti-ABCB9 (Santa Cruz biotechnology, Dallas, USA) or anti-ABCB6 antibody (Santa Cruz biotechnology, Dallas, USA) as primary antibodies and anti-mouse antibody (#R8201, ScanLater, Molecular Devices, California, USA) as the secondary antibody. **A.** Centrifugation of the S fraction of MDA-MB-231 subcellular fractionation with anti-ABCB9 antibody. A band is seen in the S fraction and in the pellet above 100 kDa. **B.** Centrifugation of the S fraction of MDA-MB-231 with anti-ABCB6, bands are detected in the S fraction, in the supernatant and in the pellet, at around 85 kDa. **C.** Centrifugation of the S fraction of MDA-MB-435 with anti-ABCB9 antibody, a band is seen in the S fraction and in the supernatant at a weight greater than 100 kDa. **D.** Centrifugation of the S fraction of MDA-MB-435 with anti-ABCB6 antibody, bands are detected in the S fraction and in the supernatant at around 70 kDa.

The additional centrifugation did not allow us to detect ABCB9 and ABCB6 only in the pellet fraction. We can see that for MDA-MB-231 cell line, ABCB9 is detected in the S fraction, and in the pellet but not in the supernatant, whereas ABCB6 is detected in all the fractions. Regarding MDA-MB-435 cell line, ABCB9 and ABCB6 are detected in the S fraction and the supernatant but not in the pellet. This could mean that the additional centrifugation for MDA-MB-435 might require higher centrifugal forces to obtain a bigger pellet. Concerning the additional centrifugation for MDA-MB-231, we can observe that both transporters are detected in the pellet, which means that perhaps microsomes can explained the presence of those transporters in the S fraction.

4.2.4 Investigation of antibody specificity

4.2.4.1 Expression of mCherry-tagged ABCB9 construct in MDA-MB-231 and MDA-MB-435 cell lines

Because ABCB6 and ABCB9 were highlighted in the fraction S and the additional centrifuge of this fraction was not able to clearly link both transporters with other organelles, it was decided to investigate both primary antibodies specificity (i.e. anti-ABCB9 and anti-ABCB6). We wanted to answer the following question, do they really recognize our proteins of interest? To do so, we decided to use an ABCB9 tagged with mcherry in order to detect ABCB9 with an anti-mCherry antibody in a western blot after fractionation and to compare the obtained results with the one on Figures 15 and 17. The first step was to test ABCB9-mCherry transfection on MDA-MB-231 cells (**Figure 19**). Thus, MDA-MB-231 cells were transfected with 2 µg of pcDNA3.1 B9-mCherry or pcDNA3.1 mCherry construct, and incubated during 48 hours before protein extraction. 5 µg of cell lysates were loaded on the western blot, which was revealed with an anti-mCherry antibody (Sicgen, Cantanhede, Portugal) using the LI-COR. The weight of the mCherry is 29 kDa and the weight of B9-mCherry is around 113 kDa.

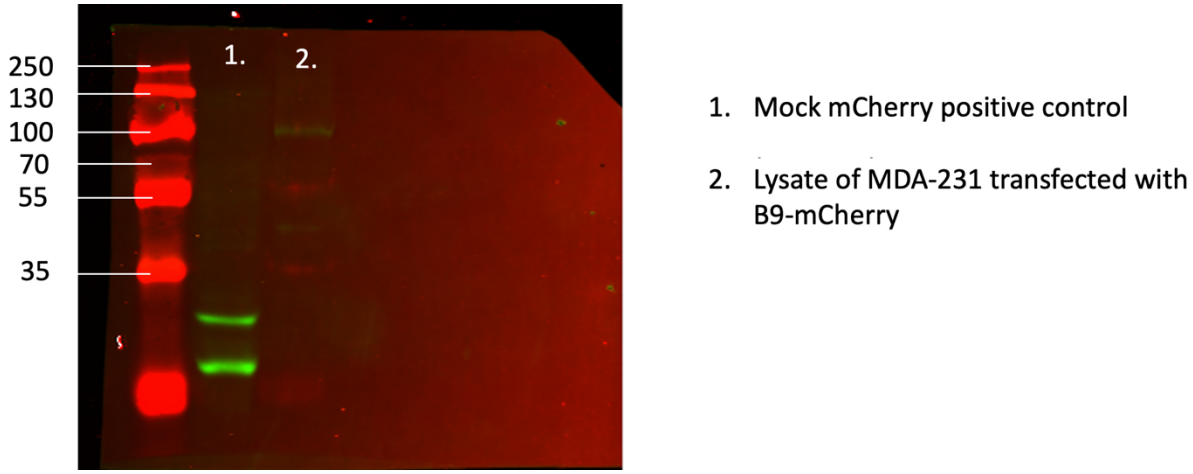

Figure 19 – Detection of mCherry and mcherry-tagged ABCB9 in MDA-MB-231 cell line. MDA-MB-231 cells were transfected with mcherry or ABCB9-mCherry construct and incubated for 48 hours. Cells were harvested and 5 µg of proteins were loaded on the gel. It was revealed using anti-mCherry antibody (Tomato, Sicgen, Cantanhede, Portugal) as the primary antibody and a donkey anti-goat (LI-COR, Lincoln, Nebraska, USA) antibody as the secondary one. Two bands are observed in the mock mCherry positive control, between 15 and 35 kDa. No bands are seen in the lysate of MDA-MB-231 cells transfected with B9-mCherry.

On the western blot in **Figure 19**, there is no band visible at the expected size for the MDA-MB-231 cells transfected with mCherry-tagged ABCB9.

To confirm that the absence of band was due to a transfection issue with the MDA-MB-231 cells, it was decided to transfect HEK293T, MDA-MB-231 and MDA-MB-435 cell lines with pCA-βeGFP and to observe them 48 hours after transfection using fluorescence microscope (Axiovert 135 TV, Oberkochen, Germany) (**Figure 20**). GFP is excited at 489 nm and emits at 509 nm.

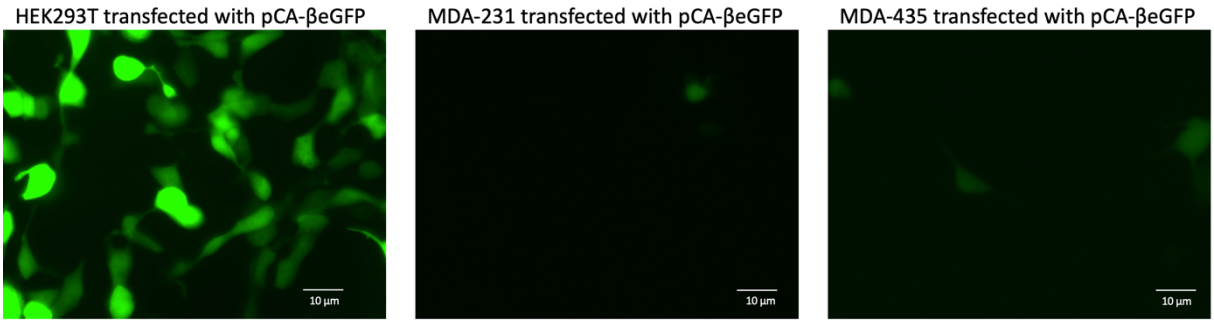

Figure 20 – Transfection of HEK293T, MDA-MB-231 and MDA-MB-435 cell lines. Cells were plated at $4x10^5$ cells/ml in a 6-well plate using the Vi-cell XR (Beckman Coulter, Brea, California USA). Cells were transfected with pCA-beGFP when they reached 60-80% of confluence and were incubated during 48 hours at 37°C 5% CO_2 before using a fluorescent microscope (Axiovert 135 TV, Oberkochen, Germany). GFP was excited at 489 nm and emitted at 509 nm which is visible in green. Pictures were taken at 10x magnification

A green signal was visible in the HEK293T cell line. However, no signal is observed for MDA-MB-231 and MDA-MB-435 cell lines (**Figure 20**). Therefore, we concluded that MDA-MB-231 and MDA-MB-435 cells have difficulties to be transfected using jetPRIME.

4.2.4.2 Inhibition of ABCB9 expression in HEK293T using shRNAs.

To move on with the analysis of ABCB9 antibody specificity, we decided to use short hairpin RNA (shRNA). The aim of the shRNA is to silence a target gene expression, in this case, ABCB9. ShRNA is an artificial RNA that is complementary to endogenous mRNA and which binds to it. As a result, it will silence the target mRNA. Because transfection in MDA-MB-231 and MDA-MB-435 cell lines was an issue (**Figure 20**), it was decided to continue with HEK293T cells. 48h after the transfection of the shRNA plasmid, proteins were extracted and loaded on a western blot to see if we notice a decrease of signal using the anti-ABCB9 antibody (Santa Cruz Biotechnology, Dallas, USA). Protein extraction was performed using 4 conditions; non-transfected HEK293T cells, HEK293T cells transfected with non-target shRNA (negative control), and HEK293T transfected with shRNA plasmid using two different transfection ratio 1:1 and 1:4. 5 µg of proteins from each condition were loaded on the western blot gel, which was revealed with anti-ABCB9 antibody (Santa Cruz Biotechnology, Dallas, USA) as primary antibody or anti-α Tubulin (Abcam, Cambridge, UK) as housekeeping protein. Anti-mouse antibody (#R8201, ScanLater, Molecular Devices, California, USA) was used for ABCB9 and anti-rabbit antibody (#R8204, ScanLater anti-rabbit, Molecular Devices, San Jose, USA) for α-Tubulin as the secondary antibodies (**Figure 21**).

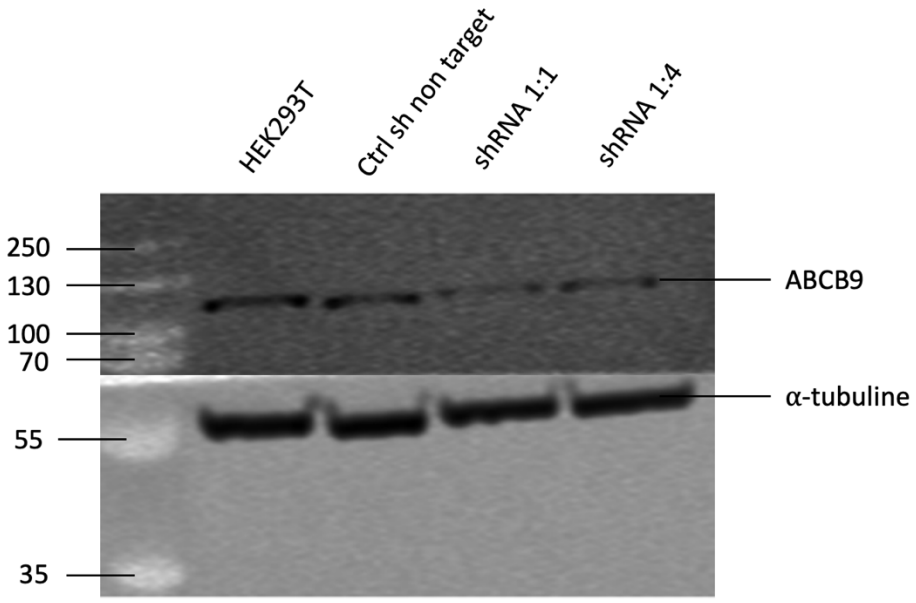

Figure 21 – Detection of ABCB9 and α-Tubulin in HEK293T cells transfected with ABCB9-targeting shRNA. HEK293T cells were plated in 6 well-plate, $2x10^5$ cells per mL. ABCB9 shRNA plasmid (Santa Cruz Biotechnology, Dallas, USA) was transfected as per the manufacturer's instructions (Santa Cruz Biotechnology, Dallas, USA). Four different conditions were used: non-transfected HEK293T cells, control non-target shRNA, HEK293T transfected with shRNA plasmid using a transfection ratio 1:1 and 1:4. Proteins were extracted from each condition and 5 µg of proteins were loaded on the gel and revealed with anti-ABCB9 antibody (Santa Cruz Biotechnology, Dallas, USA) as primary antibody and anti-mouse antibody (#R8201, ScanLater, Molecular Devices, California, USA) as the secondary antibody. The western blot reveals bands in each condition for ABCB9, the intensity is decreasing in shRNA 1:1 and shRNA 1:4. α-tubulin was used as a housekeeping protein.

Figure 21 shows ABCB9 bands in each well at a size above 100 kDa. It also shows that the intensity of the band is decreasing in the condition shRNA 1:1 and 1:4. The α-tubulin is observed at the right size of 55 kDa and is used as an internal control to ensure that the same amount of proteins was loaded in each well. The data will have to be analyzed using ImageJ to get a quantitative result of the ABCB9 silencing. Furthermore, a RT-qPCR could also be done to obtain quantitative results. This observation suggests that the anti-ABCB9 antibody (Santa Cruz Biotechnology, Dallas, USA) is specific.

4.3 Heterodimerization investigation of ABCB9 with ABCB6 using co-immunoprecipitation

Despite ABCB6 and ABCB9 expression in both MDA-MB-231 and MDA-MB-435 cell lines, their localization remains questionable. However, it was decided to investigate their possible heterodimerization using co-immunoprecipitation. The aim was to confirm preliminary data obtained in our laboratory [84, 85].

First, HEK293T cells were transfected with 2 µg of pcDNA3.1 B9-mCherry and incubated during 48 hours before protein extraction. Then, 3 different Co-IP were performed. The first one was the negative control, protein lysate prepared from HEK-293T cells transfected with B9-mCherry was precipitated by IgG. The second Co-IP used protein lysate obtained from HEK293T cells that were not transfected, which was precipitated by anti ABCB9 antibody. And the last one, protein lysate from HEK293T cells transfected with ABCB9-mCherry precipitated by anti-ABCB6 antibody. All co-immunoprecipitations were revealed by anti-mCherry antibody (Tomato, Sicgen, Cantanhede, Portugal) as the primary antibody and Donkey anti-rabbit as secondary antibody (DAG, (LI-COR, Lincoln, Nebraska, USA). A lysate of HEK293T transfected with B9 mCherry was used as a positive control (**Figure 22**). The weight of mCherry is 29 kDa and the weight of B9-mCherry is around 113 kDa. If ABCB9 heterodimerizes with ABCB6, a band at 113 kDa should be seen.

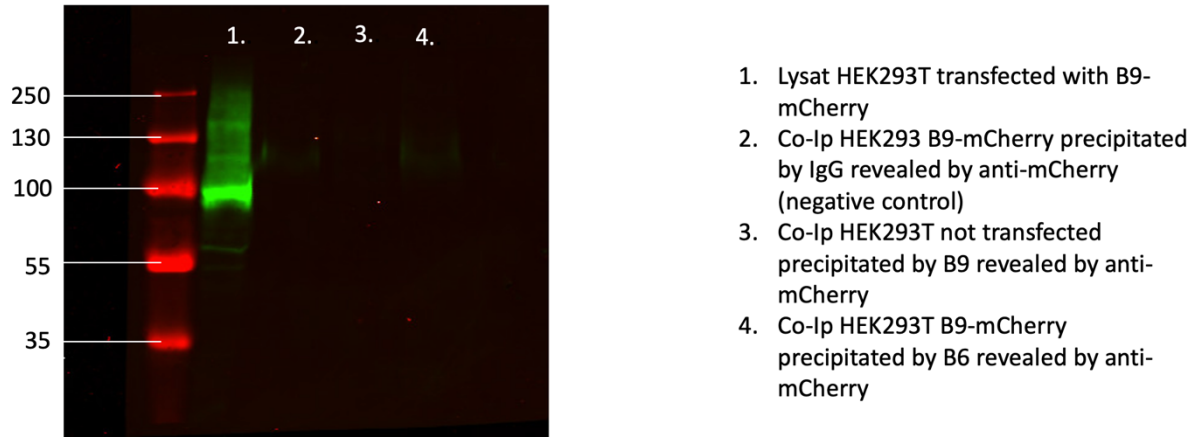

Figure 22 – Investigation of the heterodimerization of ABCB9 and ABCB6 by co-immunoprecipitation. Three co-IP were performed. In lane 2, the first co-IP was the negative control, protein lysate prepared from HEK-293T cells transfected with B9-mCherry was precipitated by IgG. In lane 3, the second co-IP used protein lysate obtained from HEK293T cells that were not transfected, which was precipitated by anti ABCB9 antibody. And the last one, in lane 4: protein lysate from HEK293T cells transfected with ABCB9-mCherry was precipitated by anti-ABCB6 antibody. All co-immunoprecipitations were revealed by anti-mCherry antibody (Tomato, Sicgen, Cantanhede, Portugal) as the primary antibody and Donkey anti-rabbit as secondary antibody (DAG, (LI-COR, Lincoln, Nebraska, USA). A lysate of HEK293T transfected with B9 mCherry was used as a positive control (Figure 22). The weight of mCherry is 29 kDa and the weight of B9-mCherry is around 113 kDa. If ABCB9 heterodimerizes with ABCB6, a band at 113 kDa should be seen.

As observed on **Figure 22**, no band is seen in the Co-IP using protein lysate prepared from HEK293T transfected with B9-mCherry, precipitated by anti-ABCB6 antibody and revealed by anti-mCherry antibody. If ABCB9 and ABCB6 did heterodimerize together, a band should be seen around 113 kDa, at the same size than the band obtained for the positive control.

We acquired a new anti-ABCB6 antibody (Rockland, Philadelphia, USA), and performed the co-IP again using HEK293T cells transfected with 2 µg of pcDNA3.1 B9-mCherry and incubated during 48 hours before protein extraction. Protein extraction was done on HEK293T

cells and 2 Co-IP were performed. In the first one, proteins were precipitated with the new anti-ABCB6 antibody, and in the second one, proteins were precipitated using IgG from rabbit (negative control). 5 µg of HEK293T lysate (positive control) was loaded on the gel along with the 2 co-IPs, and was revealed using anti-ABCB9 antibody (Santa Cruz Biotechnology, Dallas, USA) and anti-mouse (#R8201, ScanLater, Molecular Devices, California, USA) as the secondary antibody. A band around 120 kDa is seen for ABCB9 in the positive control. If ABCB9 and ABCB6 do heterodimerize, a band around 84 kDa should be observed in the first Co-IP (**Figure 23**).

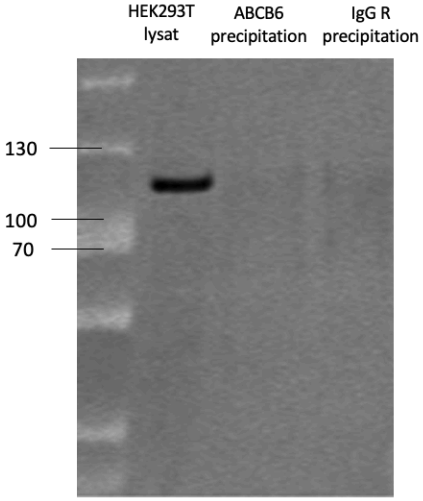

Figure 23 – Investigation of the heterodimerization of ABCB9 and ABCB6 by Co-immunoprecipitation. Co-immunoprecipitation performed by precipitation of ABCB6 followed by the revelation of ABCB9 on HEK-293T cell lines using the same conditions as the experiment presented in Figure 22.

The co-immunoprecipitation (**Figure 25**) shows a band only in the HEK293T lysate and not in the ABCB6 precipitation revealed by the anti-ABCB9 primary antibody (Santa Cruz Biotechnology, Dallas, USA). Therefore, it doesn't allow us to show the heterodimerization of ABCB9 with ABCB6.

5 Conclusion, discussion and perspectives

ABCB9 and ABCB6 are both members of the ATP-binding Cassette (ABC) transporter superfamily. They are half transporters that need to dimerize to form a full transporter in order to transport substrates across membranes. Some half transporters homodimerize, while others heterodimerize (i.e ABCB2 with ABCB3). So far, those two transporters showed that they homodimerize to function [16, 39]. However, during her master thesis, Louise Gerard showed, using the NanoBRET assay, that those two transporters could potentially heterodimerize [85]. As those results were obtained on HEK293T cells that were transfected with ABCB9 and ABCB6, my thesis aimed to validate this heterodimerization on cells that constitutively express those two transporters. Before investigating the heterodimerization, the expression and localization of ABCB9 and ABCB6 in MDA-MB-231, MDA-MB-435 and Sertoli cells were studied.

The expression of ABCB9 and ABCB6 in the chosen cell lines were studied using western blot and RT-qPCR (**Figure 13** and **Table 6**). We noticed that ABCB9 bands were higher than 100 kDa, while it was supposed to be at 84 kDa. However, Zhang *et al.* have shown that ABCB9 comprises five N-glycosylation sequence motifs [43]. If ABCB9 is indeed glycosylated, this post-translational modification could explain this higher molecular weight on the gel. To determine whether the weight of ABCB9 is increased by the N-glycosylation, a treatment using N-glycosidase F could be done prior to the western blot analysis. Regarding the ABCB6 bands, it seemed that the bands were at 68-69 kDa instead of 79 kDa, this could be explained by the aberrant behavior of highly hydrophobic proteins on SDS gels. We also observed that the Sertoli cell line did not express ABCB6 at the protein level. However, using RT-qPCR, we observed that ABCB6 was expressed at the mRNA level. This could be explained by the fact that mRNA can be repressed by microRNA, directly inhibiting mRNA translation, which results in no protein expression. Therefore, we decided to continue our research project with the MDA-MB-231 and MDA-MB-435 cell lines that both express ABCB9 and ABCB6 at the mRNA and the protein levels. Localization of ABCB6 and ABCB9 has been already discussed in many papers and remains controverted for both transporters. The localization of ABCB9 is debated either in the lysosomes or in the endoplasmic reticulum [41, 45, 46]. For ABCB6, it remains discussed between the mitochondria and in the endo-lysosomal compartment [53, 54]. Hence, we decided to study their localization using subcellular fractionation. Regarding MDA-MB-231 cell fractionation and its distribution profile (**Figure 14**), we noticed that the β-hexosaminidase (lysosome enzyme) was recovered mainly in the M fraction (37,5%) compared to the L fraction (18,8%) where it was expected. However, during his master thesis, Maxence Toussaint has shown, using immunofluorescence, that MDA-MB-231 cells exhibit very large lysosomes [90]. This could explain why lysosomes were recovered in the M fraction, they sedimented at lower speed given that they were larger. We also noticed a high enrichment of alkaline phosphodiesterase in the L fraction, which is possible if plasma membranes were broken down into larger vesicles than usual. For histone H1, a strange profile was observed as it was mainly recovered in the M fraction and the P fraction even though high enrichment is seen in the N fraction. An additional nuclear marker distribution profile should be assessed, such as histone H3, to make sure that the fractionation is reliable. This could be caused by too many passages, but the distribution profile of the other enzymes did not seem to show excessive number of passages. All distribution profiles of MDA-MB-435 cell fractionation showed the expected trend, excepted for the β-hexosaminidase (lysosome enzyme) which is recovered at 44,0% in

the P fraction and only 26,4% in the L fraction. Nevertheless, the enrichment is higher in the L fraction, lysosomes might be smaller than usual and therefore are recovered in the fraction P.

For both cell fractionations (**Figure 15 and 17**), we localized ABCB9 and ABCB6 mainly in the S fraction, which is the soluble fraction. Those transporters are transmembrane proteins, which means that they should not be in the cytosolic soluble fraction. Consequently, we did an additional centrifugation with the S fraction with the aim to pellet microsomes that could be found in the S fraction. On **Figure 18**, we see that for the MDA-MB-231 cell fractionation, ABCB9 is only detected in the pellet, which let us think that there is a possibility that it is localized in smaller microsomes (ER). ABCB6 is detected in both supernatant and pellet, which can be due to the fact that microsomes are still in the supernatant. If greater centrifugation forces were applied, perhaps all the microsomes would be recovered in the pellet. Regarding the fractionation of MDA-MB-435 cells, both ABCB6 and ABCB9 are only detected in the supernatant. As explained above, at the end of the additional centrifugation of the S fraction, a very small pellet, almost indistinguishable, was obtained. If a higher centrifugation forces were applied, recovery of both transporters could be observed in the pellet of the S fraction. However, this hypothesis is not supported by the literature, generally centrifugation of 80,000 to 100,000 g are used to recover microsomes and 200 000 g is sufficient to recover smooth microsomes, which are lighter than rough microsomes [91-93].

Another hypothesis can be done based on the work of Hiroshi Nakagawa *et al.* [94]. They showed that *ABCC11* had a non-synonymous polymorphism that affected the function and stability of ABCC11 protein production. The polymorphism affects the N-linked glycosylation of the protein, which lead to a misfold. Misfolded proteins, which accumulates in the ER are removed from it, by retro-translocation, into the cytosol compartment and finally are degraded by the ubiquitin-proteasome system [94, 95]. ABCB9 and ABCB6 both contains N-glycosylation sites, hence, if they are N-glycosylated, a polymorphism could occur and affect their folding [16, 43]. To study potential polymorphisms in *ABCB9* and *ABCB6*, DNA sequencing, such as Illumina or ion torrent can be done for both cell lines (i.e MDA-MB-231 and MDA-MB-435).

Another study, carried out on *C19orf12*, which encode a mitochondrial membrane protein, has shown that G58S mutation located in the transmembrane domain was affecting a glycine residue of the glycine zipper motifs [96]. This motif is involved in dimerization of transmembrane helices and is predicted to be involved in the impaired localization of the protein. Indeed, this protein is usually detected in the mitochondria, ER and mitochondria associated membranes. However, the mutant of C19orf12 was found in the cytosol. We could hypothesize that a mutation occurring in TMD0, which is suspected to target both ABCB6 and ABCB9 in the lysosome is responsible for the impair localization in the cytosol [16, 39]. Further *in silico* studies on ABCB9 and ABCB6, using MEMSAT3 for example, should be performed to identify motifs that could be involved in their potentially impaired localization.

Additional experiments could be done to further investigate the localization of these proteins. Immunofluorescence could be performed to co-localize ABCB9 and ABCB6 with specific organelle markers (ER-tracker, LAMP1, mitotracker, etc.). Another interesting experiment to do, would be to perform the fractionation on HEK293T cells, which are not cancerous cells, to determine whether the ABCB9 and ABCB6 profiles are similar to the ones obtained in cancer cells.

During the validation of the specificity of the anti-ABCB9 antibody, we highlighted a transfection issue with the MDA-MB-231 and MDA-MB-435 cell lines using JetPrime. Another transfection technique could be used, such as electroporation, which showed a good

transfection of mCherry in MDA-MB-231 cell line [97]. However, we continued the investigation by using shRNA. The western blot in **Figure 21** showed a decrease of the ABCB9 protein expression, which indicate that the anti-ABCB9 antibody (Santa Cruz Biotechnology, Dallas, USA) is specific. Nonetheless, a quantitative analysis of the band remains to be performed using the ImageJ software.

Finally, we investigated the heterodimerization of ABCB9 and ABCB6 in HEK293T cells using co-immunoprecipitation (**Figure 22 and 23**). Unfortunately, we could not demonstrate heterodimerization between those two transporters. An additional positive control should be done by revealing the western blot (**Figure 25**) with the anti-ABCB6 antibody to make sure that the antibody did bind to the beads during Co-IP. This experiment also needs to be done on MDA-MB-231 and MDA-MB-435 cell lines as ABC transporters expression and function vary across cell type. The heterodimerization could have been studied using others methods, such as the Proximity Ligation Assay (PLA). This method consists of using 2 different primary antibodies from different species to detect the two targeted proteins. Then a pair of secondary antibodies, which are labeled with oligonucleotide (PLA probes) binds to the primary antibodies. A hybridizing connector oligo joins to the PLA probes if they are in close proximity to each other. A ligase will form a closed circular DNA template, with the PLA probes, that will be amplified. Finally, a labeled oligo will hybridize to the complementary sequences within the amplicon, which can be visualized using a microscope [98].

In conclusion, we could not show the heterodimerization of ABCB9 with ABCB6 in HEK293T cells. The results obtained by NanoBRET could not be validated. Localization of ABCB9 and ABCB6 remains controverted but our data pinpointed some technical issues that are being resolved and allowed us to proposed additional experiments, which we hope will contribute to unravel the localization of both transporters and to determine whether these two transporters may really heterodimerize.

Appendices

	M	L	P
ml	8000RPM	25000RPM	35000RPM
2	2'24"	2'52"	18'30"
2,1	2'27"	2'54"	
2,2	2'30"	2'56"	
2,3	2'33"	2'59"	
2,4	2'36"	3'02"	
2,5	2'39"	3'04"	
2,6	2'42"	3'06"	
2,7	2'45"	3'09"	
2,8	2'48"	3'11"	
2,9	2'52"	3'13"	
3	2'55"	3'16"	21'40"
3,1	2'59"	3'19"	
3,2	3'03"	3'22"	
3,3	3'07"	3'25"	
3,4	3'11"	3'28"	
3,5	3'15"	3'31"	
3,6	3'19"	3'34"	
3,7	3'23"	3'37"	
3,8	3'27"	3'40"	
3,9	3'31"	3'42"	
4	3'34"	3'45"	24'20"
4,1	3'38"	3'48"	
4,2	3'42"	3'51"	
4,3	3'46"	3'54"	
4,4	3'50"	3'57"	
4,5	3'54"	4'	
4,6	3'58"	4'03"	
4,7	4'02"	4'07"	
4,8	4'06"	4'10"	
4,9	4'11"	4'13"	
5	4'15"	4'16"	28'20"
5,1	4'18"	4'19"	
5,2	4'21"	4'22"	
5,3	4'24"	4'25"	
5,4	4'26"	4'29"	
5,5	4'29"	4'32"	
5,6	4'31"	4'35"	
5,7	4'34"	4'38"	
5,8	4'37"	4'42"	
5,9	4'40"	4'45"	
6	4'43"	4'48"	32'13"

Appendix 1 – Centrifugation times in the 70Ti rotor depending on the fraction and the sample's volume

Bibliography

1. Robey, R.W., et al., *Revisiting the role of ABC transporters in multidrug-resistant cancer.* Nat Rev Cancer, 2018. **18**(7): p. 452-464.
2. Dean, M., A. Rzhetsky, and R. Allikmets, *The human ATP-binding cassette (ABC) transporter superfamily.* Genome Res, 2001. **11**(7): p. 1156-66.
3. Wilkens, S., *Structure and mechanism of ABC transporters.* F1000Prime Rep, 2015. **7**: p. 14.
4. Chang, G., *Multidrug resistance ABC transporters.* FEBS Letters, 2003. **555**(1): p. 102-105.
5. Pasello, M., A.M. Giudice, and K. Scotlandi, *The ABC subfamily A transporters: Multifaceted players with incipient potentialities in cancer.* Semin Cancer Biol, 2020. **60**: p. 57-71.
6. Vasilis Vasiliou, K.V.a.D.W.N., *Human ATP-binding cassette (ABC) transporter family.* 2009.
7. Velamakanni, S., et al., *ABCG transporters: structure, substrate specificities and physiological roles : a brief overview.* J Bioenerg Biomembr, 2007. **39**(5-6): p. 465-71.
8. Linton, K.J., *Structure and function of ABC transporters.* Physiology (Bethesda), 2007. **22**: p. 122-30.
9. Gillet, J.P., T. Efferth, and J. Remacle, *Chemotherapy-induced resistance by ATP-binding cassette transporter genes.* Biochim Biophys Acta, 2007. **1775**(2): p. 237-62.
10. Michael M. Gottesman, S.V.A., *Overview: ABC Transporters and Human Disease.* Journal of Bioenergetics and Biomembranes, 2001.
11. Domenichini, A., A. Adamska, and M. Falasca, *ABC transporters as cancer drivers: Potential functions in cancer development.* Biochim Biophys Acta Gen Subj, 2019. **1863**(1): p. 52-60.
12. Oswald, C., I.B. Holland, and L. Schmitt, *The motor domains of ABC-transporters. What can structures tell us?* Naunyn Schmiedebergs Arch Pharmacol, 2006. **372**(6): p. 385-99.
13. Hofmann, S., et al., *Conformation space of a heterodimeric ABC exporter under turnover conditions.* Nature, 2019. **571**(7766): p. 580-583.
14. Chen, Y.K.a.J., *Molecular structure of human P-glycoprotein in the ATP-bound, outward-facing conformation.* Science, 2018.
15. Tusnady, G.E., et al., *Membrane topology of human ABC proteins.* FEBS Lett, 2006. **580**(4): p. 1017-22.
16. Boswell-Casteel, R.C., Y. Fukuda, and J.D. Schuetz, *ABCB6, an ABC Transporter Impacting Drug Response and Disease.* AAPS J, 2017. **20**(1): p. 8.
17. Graab, P., et al., *Lysosomal targeting of the ABC transporter TAPL is determined by membrane-localized charged residues.* J Biol Chem, 2019. **294**(18): p. 7308-7323.
18. Genovese, I., et al., *Not only P-glycoprotein: Amplification of the ABCB1-containing chromosome region 7q21 confers multidrug resistance upon cancer cells by coordinated overexpression of an assortment of resistance-related proteins.* Drug Resist Updat, 2017. **32**: p. 23-46.
19. Fukuda, Y., et al., *The severity of hereditary porphyria is modulated by the porphyrin exporter and Lan antigen ABCB6.* Nat Commun, 2016. **7**: p. 12353.
20. Yoo, E.G., *Sitosterolemia: a review and update of pathophysiology, clinical spectrum, diagnosis, and management.* Ann Pediatr Endocrinol Metab, 2016. **21**(1): p. 7-14.
21. Patel, S.B., G.A. Graf, and R.E. Temel, *ABCG5 and ABCG8: more than a defense against xenosterols.* J Lipid Res, 2018. **59**(7): p. 1103-1113.

22. Ling, R.L.J.a.V., *A surface glycoprotein modulating drug permeability in chinese hamster ovary cell mutants.* 1976.
23. C G Dietrich, A.G., R P J Oude Elferink, *ABC of oral bioavailability : transporters as gatekeepers in the gut* 2003.
24. Sharom, F.J., *ABC proteins : From Bacteria to Man* Elsevier Science. Vol. Chaper 6 : Probing og conformational changes, catalytic cycle and ABC transporter function. 2003.
25. Sticova, E. and M. Jirsa, *ABCB4 disease: Many faces of one gene deficiency.* Ann Hepatol, 2020. **19**(2): p. 126-133.
26. Guo, Q., et al., *ATP-binding cassette member B5 (ABCB5) promotes tumor cell invasiveness in human colorectal cancer.* J Biol Chem, 2018. **293**(28): p. 11166-11178.
27. Vasquez-Moctezuma, I., et al., *ATP-binding cassette transporter ABCB5 gene is expressed with variability in malignant melanoma.* Actas Dermosifiliogr, 2010. **101**(4): p. 341-8.
28. Yang, J.Y., et al., *p-Glycoprotein ABCB5 and YB-1 expression plays a role in increased heterogeneity of breast cancer cells: correlations with cell fusion and doxorubicin resistance.* BMC Cancer, 2010. **10**: p. 388.
29. Chen, K.G., et al., *Principal expression of two mRNA isoforms (ABCB 5alpha and ABCB 5beta) of the ATP-binding cassette transporter gene ABCB 5 in melanoma cells and melanocytes.* Pigment Cell Res, 2005. **18**(2): p. 102-12.
30. Setia, N., et al., *Profiling of ABC transporters ABCB5, ABCF2 and nestin-positive stem cells in nevi, in situ and invasive melanoma.* Mod Pathol, 2012. **25**(8): p. 1169-75.
31. Moitra, K., et al., *Molecular evolutionary analysis of ABCB5: the ancestral gene is a full transporter with potentially deleterious single nucleotide polymorphisms.* PLoS One, 2011. **6**(1): p. e16318.
32. Frank, N.Y. and M.H. Frank, *ABCB5 gene amplification in human leukemia cells.* Leuk Res, 2009. **33**(10): p. 1303-5.
33. Kondo, S., et al., *Upregulation of cellular glutathione levels in human ABCB5- and murine Abcb5-transfected cells.* BMC Pharmacol Toxicol, 2015. **16**: p. 37.
34. Kawanobe, T., et al., *Expression of human ABCB5 confers resistance to taxanes and anthracyclines.* Biochem Biophys Res Commun, 2012. **418**(4): p. 736-41.
35. Keniya, M.V., et al., *Drug resistance is conferred on the model yeast Saccharomyces cerevisiae by expression of full-length melanoma-associated human ATP-binding cassette transporter ABCB5.* Mol Pharm, 2014. **11**(10): p. 3452-62.
36. Liesa, M., W. Qiu, and O.S. Shirihai, *Mitochondrial ABC transporters function: the role of ABCB10 (ABC-me) as a novel player in cellular handling of reactive oxygen species.* Biochim Biophys Acta, 2012. **1823**(10): p. 1945-57.
37. Seguin, A. and D.M. Ward, *Mitochondrial ABC Transporters and Iron Metabolism.* Journal of Clinical & Experimental Pathology, 2018. **08**(01).
38. Chen, R., et al., *Role of polymorphic bile salt export pump (BSEP, ABCB11) transporters in anti-tuberculosis drug-induced liver injury in a Chinese cohort.* Sci Rep, 2016. **6**: p. 27750.
39. Zhao, C., et al., *Peptide specificity and lipid activation of the lysosomal transport complex ABCB9 (TAPL).* J Biol Chem, 2008. **283**(25): p. 17083-91.
40. Zollmann, T., et al., *Single liposome analysis of peptide translocation by the ABC transporter TAPL.* Proc Natl Acad Sci U S A, 2015. **112**(7): p. 2046-51.
41. Ayako Kobayashi, M.K., * Tatsuo Maeda,* Shin-ichiro Hori," Kiyoto Motojima/ 1, T. MikioSuzuki, *Ei-ichiTakahashi,*IbahioYabe, KeyiTanaka,• 14, and Y. MasanoriKasahara, *andMasatomoMaeda', *A Half-Type ABC Transporter TAPL Is Highly Conserved between Rodent and Man, and the Human Grene Is Not Responsive to Interferon-7 in Contrast to TAPl and TAP21.* 2000.

42. Kobayashi, A., et al., *Gene organization of human transporter associated with antigen processing-like (TAPL, ABCB9): analysis of alternative splicing variants and promoter activity.* Biochem Biophys Res Commun, 2003. **309**(4): p. 815-22.
43. Zhang, F., et al., *Characterization of ABCB9, an ATP binding cassette protein associated with lysosomes.* J Biol Chem, 2000. **275**(30): p. 23287-94.
44. Wolters, J.C., R. Abele, and R. Tampe, *Selective and ATP-dependent translocation of peptides by the homodimeric ATP binding cassette transporter TAP-like (ABCB9).* J Biol Chem, 2005. **280**(25): p. 23631-6.
45. Ayako Kobayashi, T.M., and Masatomo MAEDA, *Membrane Localization of Transporter Associated with Antigen Processing (TAP)-Like (ABCB9) Visualized in Vivo with a Fluorescence Protein-Fusion Technique.* 2004.
46. Bock, C., et al., *Structural and functional insights into the interaction and targeting hub TMD0 of the polypeptide transporter TAPL.* Sci Rep, 2018. **8**(1): p. 15662.
47. Demirel, O., et al., *Tuning the cellular trafficking of the lysosomal peptide transporter TAPL by its N-terminal domain.* Traffic, 2010. **11**(3): p. 383-93.
48. Que, K.T., et al., *MicroRNA-31-5p regulates chemosensitivity by preventing the nuclear location of PARP1 in hepatocellular carcinoma.* J Exp Clin Cancer Res, 2018. **37**(1): p. 268.
49. Gong, J.P., et al., *Overexpression of microRNA-24 increases the sensitivity to paclitaxel in drug-resistant breast carcinoma cell lines via targeting ABCB9.* Oncol Lett, 2016. **12**(5): p. 3905-3911.
50. Hlavata, I., et al., *The role of ABC transporters in progression and clinical outcome of colorectal cancer.* Mutagenesis, 2012. **27**(2): p. 187-96.
51. Katryn N. Furuya, G.B., Daxi Sun, Erin G. Schuetz, and John D. Schuetz, *Identification of a New P-glycoprotein-like ATP-binding Cassette Transporter Gene That Is Overexpressed during Hepatocarcinogenesis.* Cancer research 1997.
52. Noboru Mitsuhashi, T.M., Hiroshi Senbongi, Norihide Yokoi, Hideki Yano, Masaru Miyazaki?, Nobuyuki Nakajima?, Toshihiko Iwanaga, Yuji Yokoyama, Takehiko Shibata, and Susumu Seino, *MTABC3, a Novel Mitochondrial ATP-binding Cassette Protein Involved in Iron Homeostasis.* 2000.
53. Jill K. Paterson, S.S., Chelsea M. Black, Tokushi Tachiwada, Susan Garfield, Stephen Wincovitch,David N. Ernst, Anissa Agadir, Xuelin Li, Suresh V. Ambudkar, Gergely Szakacs, Shin-ichi Akiyama, and Michael M. Gottesman, *Human ABCB6 Localizes to Both the Outer Mitochondrial Membrane and the Plasma Membrane.* 2007.
54. Kiss, K., et al., *Shifting the paradigm: the putative mitochondrial protein ABCB6 resides in the lysosomes of cells and in the plasma membrane of erythrocytes.* PLoS One, 2012. **7**(5): p. e37378.
55. Park, S., et al., *Gene expression profiling of ATP-binding cassette (ABC) transporters as a predictor of the pathologic response to neoadjuvant chemotherapy in breast cancer patients.* Breast Cancer Res Treat, 2006. **99**(1): p. 9-17.
56. Zheng, H.C., *The molecular mechanisms of chemoresistance in cancers.* Oncotarget, 2017. **8**(35): p. 59950-59964.
57. Mansoori, B., et al., *The Different Mechanisms of Cancer Drug Resistance: A Brief Review.* Adv Pharm Bull, 2017. **7**(3): p. 339-348.
58. Gottesman, M.M., et al., *Toward a Better Understanding of the Complexity of Cancer Drug Resistance.* Annu Rev Pharmacol Toxicol, 2016. **56**: p. 85-102.
59. Housman, G., et al., *Drug resistance in cancer: an overview.* Cancers (Basel), 2014. **6**(3): p. 1769-92.
60. Kim, S., et al., *Heterogeneity of genetic changes associated with acquired crizotinib resistance in ALK-rearranged lung cancer.* J Thorac Oncol, 2013. **8**(4): p. 415-22.

61. Rathore, R., et al., *Overcoming chemotherapy drug resistance by targeting inhibitors of apoptosis proteins (IAPs).* Apoptosis, 2017. **22**(7): p. 898-919.
62. Li, X., et al., *Autophagy: A novel mechanism of chemoresistance in cancers.* Biomed Pharmacother, 2019. **119**: p. 109415.
63. Holohan, C., et al., *Cancer drug resistance: an evolving paradigm.* Nat Rev Cancer, 2013. **13**(10): p. 714-26.
64. Yao, Z., et al., *TGF-beta IL-6 axis mediates selective and adaptive mechanisms of resistance to molecular targeted therapy in lung cancer.* Proc Natl Acad Sci U S A, 2010. **107**(35): p. 15535-40.
65. Begicevic, R.R. and M. Falasca, *ABC Transporters in Cancer Stem Cells: Beyond Chemoresistance.* Int J Mol Sci, 2017. **18**(11).
66. Bukowski, K., M. Kciuk, and R. Kontek, *Mechanisms of Multidrug Resistance in Cancer Chemotherapy.* Int J Mol Sci, 2020. **21**(9).
67. Renata Lehn Linardi, C.C.N., *Multi-drug resistance (MDR1) gene and P-glycoprotein influence on pharmacokinetic and pharmacodynamic of therapeutic drugs* 2006.
68. Lu, J.F., D. Pokharel, and M. Bebawy, *MRP1 and its role in anticancer drug resistance.* Drug Metab Rev, 2015. **47**(4): p. 406-19.
69. Wei Mo, J.-T.Z., *Human ABCG2: structure, function, and its role in multidrug resistance.* 2012.
70. Young Hee Choi, A.-M.Y., *ABC Transporters in Multidrug Resistance and Pharmacokinetics, and Strategies for Drug Development.* Current Pharmaceutical design 2014.
71. Fletcher, J.I., et al., *ABC transporters in cancer: more than just drug efflux pumps.* Nat Rev Cancer, 2010. **10**(2): p. 147-56.
72. Stefan, S.M., *Multi-target ABC transporter modulators: what next and where to go?* Future Med Chem, 2019. **11**(18): p. 2353-2358.
73. Tamaki, A., et al., *The controversial role of ABC transporters in clinical oncology.* Essays Biochem, 2011. **50**(1): p. 209-32.
74. Tang Liu, Z.L., Qing Zhang, Karen De Amorim Bernstein, Santiago Lozano-Calderon, Edwin Choy, Francis J. Hornicek, Zhenfeng Duan, *Targeting ABCB1 (MDR1) in multi-drug resistant osteosarcoma cells using the CRISPR-Cas9 system to reverse drug resistance.* Oncotarget, 2016.
75. Muriithi, W., et al., *ABC transporters and the hallmarks of cancer: roles in cancer aggressiveness beyond multidrug resistance.* Cancer Biol Med, 2020. **17**(2): p. 253-269.
76. Mochida, Y., et al., *The role of P-glycoprotein in intestinal tumorigenesis: disruption of mdr1a suppresses polyp formation in Apc(Min/+) mice.* Carcinogenesis, 2003. **24**(7): p. 1219-24.
77. Vander Borght, S., et al., *Expression of multidrug resistance-associated protein 1 in hepatocellular carcinoma is associated with a more aggressive tumour phenotype and may reflect a progenitor cell origin.* Liver Int, 2008. **28**(10): p. 1370-80.
78. Karl E. Miletti-Gonzalez, S.C., Neelakandan Muthukumaran, Giuseppa N. Saglimbeni, Xiaohua Wu, Jinming Yang, Kevin Apolito, Weichung J. Shih, William N. Hait and Lorna Rodriguez-Rodriguez, *The CD44 Receptor Interacts with P-Glycoprotein to Promote Cell Migration and Invasion in Cancer.* 2005.
79. Gong, W., et al., *Downregulation of ABCG2 protein inhibits migration and invasion in U251 glioma stem cells.* Neuroreport, 2014. **25**(8): p. 625-32.
80. Rocco, A., et al., *MDR1-P-glycoprotein behaves as an oncofetal protein that promotes cell survival in gastric cancer cells.* Lab Invest, 2012. **92**(10): p. 1407-18.

81. Sana, G., et al., *Exome Sequencing of ABCB5 Identifies Recurrent Melanoma Mutations that Result in Increased Proliferative and Invasive Capacities.* J Invest Dermatol, 2019. **139**(9): p. 1985-1992 e10.
82. Tian, C., et al., *ABCG1 as a potential oncogene in lung cancer.* Exp Ther Med, 2017. **13**(6): p. 3189-3194.
83. Wilson, B.J., et al., *ABCB5 maintains melanoma-initiating cells through a proinflammatory cytokine signaling circuit.* Cancer Res, 2014. **74**(15): p. 4196-207.
84. Simon Lefèvre, L.D., Jean-Pierre Gillet, *Co-immunoprecipitation revealed the heterodimerization of the melanoma-associated ABCB5 transporter with ABCB6 and ABCB9. Set up of a High Five insect cells expression model to determine their physiological substrates.* 2017.
85. Louise Gerard, L.D., Camille Perdrau, Marie Fourrez, Jean-Pierre Gillet, *Study of the Heterodimerization of ABCB5β with ABCB6 and ABCB9 Using NanoBRET Assay.* 2019.
86. Prasad, V.V. and R.O. Gopalan, *Continued use of MDA-MB-435, a melanoma cell line, as a model for human breast cancer, even in year, 2014.* NPJ Breast Cancer, 2015. **1**: p. 15002.
87. Rae, J.M., et al., *MDA-MB-435 cells are derived from M14 melanoma cells--a loss for breast cancer, but a boon for melanoma research.* Breast Cancer Res Treat, 2007. **104**(1): p. 13-9.
88. Banda, M., et al., *Evaluation and validation of housekeeping genes in response to ionizing radiation and chemical exposure for normalizing RNA expression in real-time PCR.* Mutat Res, 2008. **649**(1-2): p. 126-34.
89. C. De Duve, B.C.P., R. Gianetto, R. Wattiaux and F. Appelmans *Tissue Fractionation Studies 6. Intracellular distribution patterns of enzymes in rat-liver tissue* 1955.
90. Toussaint, M., *Analysis of a mannose-6-phosphorylation defect in breast cancer cells: causes, consequences on lysosomal functions and on cancer cell aggressiveness.* 2020.
91. Vrbanac, J. and R. Slauter, *ADME in Drug Discovery*, in *A Comprehensive Guide to Toxicology in Preclinical Drug Development*. 2013. p. 3-30.
92. M. R. Adelman, G.B., and David D. Sabatini, *An improved cell fractionation procedure for the preparation of rat liver membrane bound ribosomes.* 1973.
93. Jeppesen, D.K., et al., *Comparative analysis of discrete exosome fractions obtained by differential centrifugation.* J Extracell Vesicles, 2014. **3**: p. 25011.
94. Nakagawa, H., et al., *Ubiquitin-mediated proteasomal degradation of ABC transporters: a new aspect of genetic polymorphisms and clinical impacts.* J Pharm Sci, 2011. **100**(9): p. 3602-19.
95. Bonifacino, J.S. and A.M. Weissman, *Ubiquitin and the control of protein fate in the secretory and endocytic pathways.* Annu Rev Cell Dev Biol, 1998. **14**: p. 19-57.
96. Venco, P., et al., *Mutations of C19orf12, coding for a transmembrane glycine zipper containing mitochondrial protein, cause mis-localization of the protein, inability to respond to oxidative stress and increased mitochondrial Ca(2)(+).* Front Genet, 2015. **6**: p. 185.
97. Mukherjee, P., et al., *Combined Numerical and Experimental Investigation of Localized Electroporation-Based Cell Transfection and Sampling.* ACS Nano, 2018. **12**(12): p. 12118-12128.
98. Alam, M.S., *Proximity Ligation Assay (PLA).* Curr Protoc Immunol, 2018. **123**(1): p. e58.